Developing metabolomics for a systems biology approach to understand Parkinson's disease

Willacey, C.C.W.

Chapter 4

A quantitative atlas of metabolites across regions of the rat brain

Cornelius C W Willacey, Maria E Secci, Marcus W Meinhardt, Tom Schilperoord, Isabelle Kohler, Amy C Harms, Naama Karu[#], Wolfgang H Sommer[#] and Thomas Hankemeier[#]

Submitted

[#] Authors equally contributed to the manuscript

Abstract

The mammalian brain is an extremely complex organ, comprising of a multitude of regions with varying functionalities as well as genome, transcriptome, proteome and metabolome profiles. Despite the expanding research of the brain and the advancing analytical technology, quantitative metabolic mapping of the brain is rather limited. Here, we present a brain quantitative metabolic atlas of the healthy adult rat (n=16), a preferred animal model for human brain research. The atlas provides absolute quantitative values for 43 metabolites that are of biochemical importance in the brain or are associated with CNS health conditions. They represent several chemical classes, and include amino acids and neuroactive derivatives such as major neurotransmitters, polyamines, and antioxidants. We used a pre-column benzoyl chloride derivatization followed by UPLC-MS/MS analysis to accurately and sensitively measure the regions. While the current metabolic coverage is a demonstrator for the applicability of the analytical method, it can be further modified to include more metabolites of interest, taking advantage of the simple stabilisation of metabolites that are vulnerable to degradation. The quantified metabolites across 25 brain regions reflected the specialised function of several regions, showing high agreement between distinct neural composition and neurotransmitter abundance within the cells. As a proof of concept for biochemical interpretation, significant patterns were also highlighted along the metabolic pathways of tyrosine, tryptophan, urea and polyamine production. The metabolic atlas reference dataset can be further utilised as quantitative reference levels to compare to new studies and identify perturbations in relevant pathways or diseases. The dataset can also be integrated into genome-scale metabolic models, to further define neuronal networks and the connectome.

Synopsis

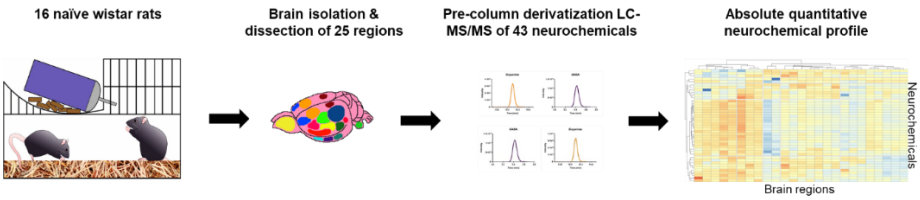

To provide metabolic reference values of the brain that can contribute to our understanding of the cellular homeostasis network and neural communication, neurochemicals were analysed in 25 brain regions from 16 healthy adult Wistar rats. To achieve this, we performed liquid-liquid extraction followed by pre-column derivatization with benzoyl chloride with UPLC-MS/MS.

- Absolute quantitation on 43 neurochemicals was performed.
- Key metabolic pathways were covered such as the tyrosine, polyamine, urea cycle and tryptophan metabolism.
- A distinct metabolic profile was identified between regions of the brain.
- The neurochemicals quantified are associated with a range of neurological disorders.
- Reference values have been provided for clinical use and metabolic model integration using a systems approach.

Background

Metabolomics has the potential to decipher the contributing factors towards diseases of the CNS [1-3] via the study of homeostasis, cell signalling, oxidative stress and communication [4]. The mammalian brain is the most complex organ, and it operates by an intricate, interconnected and synergistic network via chemical neurotransmission with localised regions designated for specific and specialised roles. In turn, some regions have a more distinct genome, transcriptome, proteome and metabolome and higher expression of specific neurons. With recent advancements in metabolomics-based technologies, it is possible to further explore the molecular phenotype of each brain region. Leading databases such as KEGG [5], BioCyc [6], and VMH [7], relate metabolic pathways to the genome, transcriptome and proteome, to understand cellular function, mechanism of diseases and therapeutic target sites [8]. Although, there has been continuous discussion about limited knowledge on the metabolic composition of the mammalian brain [9,10] followed by a noticeable absence of quantitative metabolomics data [11,4]. The majority of quantitative reference data is curated for blood, cerebrospinal fluid, and urine [12,13]. The lack of organ-specific reference data hinders the next step in research, particularly when attempting to combine data to constraint-based models. For obvious reasons, healthy human brain metabolomics work is not possible. Nevertheless, even in murine models, several of the approaches to capture the brain metabolome have focused on specific diseases or measured limited regions with minimal sensitivity for important neurotransmitters [9,14,15]. Quantitative measurement of amino acids has provided useful information but this alone does not detail the communication profile, i.e., neurotransmitters. Furthermore, this approach was also limited to the analysis of the prefrontal cortex, striatum, hippocampus and cerebellum [16]. A more practical approach to explore the brain utilises measurements of the cerebrospinal fluid [17-19]. This has been important in the detection and understanding of key metabolites associated with human diseases, but is only indicative of the brain metabolome as a whole. One of the studies that addresses this limitation comes from Choi et al. (2018)[20] who mapped the mouse brain using quantitative analysis of amino acids, lipids, peptides, nucleotides, etc. to investigate the four brain regions; frontal cortex, hippocampus, cerebellum, and olfactory bulb. Moreover, global metabolomics has been utilised to map eight mouse-derived brain

regions [4] without reporting absolute quantitative concentrations, hampering the use of this information in mechanistic models.

In this study, we developed and optimized a method for the analysis of neurometabolites in rat brain tissue based on sample derivatization with benzoyl chloride [21]. Due to the relatively high instability of neurotransmitters, specifically the catecholamines in the extracellular environment, [22], samples were derivatized to stabilise the metabolites while increasing the overall analytical sensitivity and chromatographic performance.

The developed method has led to the most comprehensive, quantitative metabolic neurochemical profile of the rat brain to date in terms of brain regions measured (n = 25), number of animals (n = 16) and metabolites absolutely quantified (n = 43). The concentration profile of 43 neurochemicals was conducted across the cerebral cortex, striatum, diencephalon, midbrain and pons. Furthermore, we focused on neurochemicals which are of interest in the research of CNS activity and diseases. We also documented the essential regions associated with the key brain pathways for control of emotion, behaviour, memory and movement, such as mesolimbic, limbic and nigrostriatal. Our atlas lays the groundwork for quantitative data integration into metabolic models which can vastly improve understanding of the functionality and pathophysiology of the mammalian brain.

Results

Metabolic profile of healthy rat brain

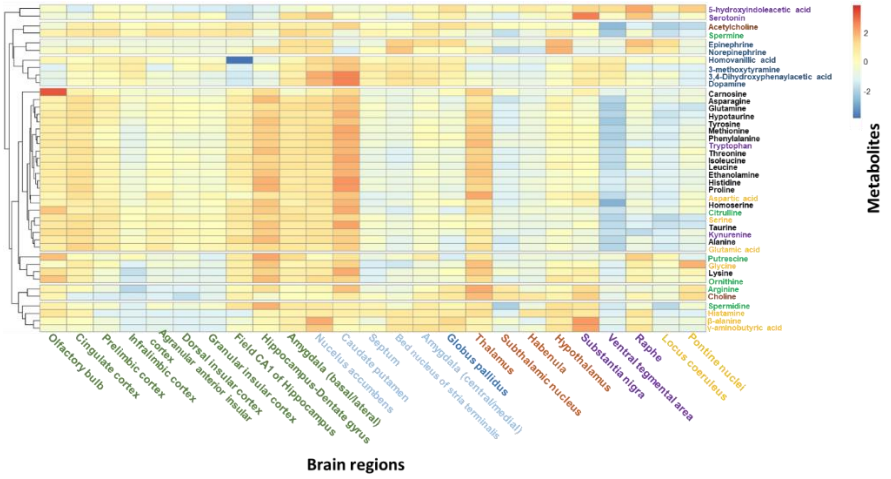

Figure 4.1: Neurochemical metabolome of healthy rodent brains. The column represents each individual brain region and the row represents the metabolites quantified. Due to the large number of brain regions, the median concentration values between the 16 samples are shown. The brain regions have been arranged by their bregma coordinates from the frontal lobe to the brain stem. The data has been clustered based on their metabolite concentration similarity using hierarchical clustering with complete linkage. The brain regions are coloured by their associated hierarchy: green, cortex; light blue, striatum; blue, pallidum; orange, diencephalon; purple, midbrain; yellow, pons. The figure is scaled using z-score across the metabolites: red represents a high concentration of the metabolite and blue represents a low concentration of metabolites. The metabolites are coloured by their associated metabolic pathways: purple, tryptophan metabolism; brown, cholinergic metabolism; blue, tyrosine metabolism; yellow, neuroactive amines; green, urea cycle and polyamine metabolism; black, biogenic amines.

Figure 4.1 provides an overview of median metabolite concentrations across the brain regions (n=25), via a heatmap of all quality-approved compounds (n=43) in the rat samples (n=16). The metabolite concentration values are reported for each rat in Tables S8-12. Hierarchical clustering with complete linkage created seven main clusters of closely-associated metabolites: serotonin and its turnover product 5-

HIAA; acetylcholine and spermine; norepinephrine and its turnover product epinephrine; dopamine metabolism into 3-MT, DOPAC and HVA; amino acids and derivatives (possibly driven by concentration similarity); ornithine and its derivative putrescine, together with glycine and lysine; arginine and choline; histamine, spermidine, β-alanine and GABA (all neuroactive). The brain regions in the presented heatmap are arranged by parent regions based on physical proximity. When hierarchical clustering of the brain regions was performed according to the metabolic profile (Fig. S2), some of the formed clusters corresponded with the parent regions (e.g. insular regions as part of the cortex). The clustering of brain regions is also demonstrated in a unsupervised analysis using principal component analysis (Fig. S1).

Neurotransmitter abundance across the brain

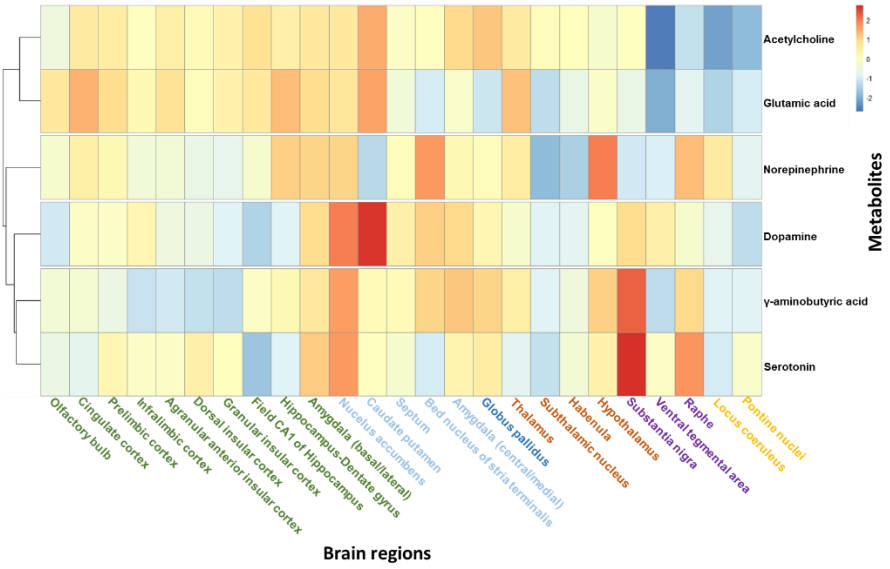

Figure 4.2: Heat map showing the relative concentrations of acetylcholine, glutamate, norepinephrine, serotonin, dopamine and GABA across all 25 brains regions. The heat map has been arranged by the distance from the bregma coordinates and clustered by metabolite concentration similarity. The figure is scaled using z-score to identify the movement from the mean across the metabolites: red represents a high concentration of the metabolites and blue represents a low concentration of metabolites. The brain

regions are coloured by their associated hierarchy: green, cortex; light blue, striatum; blue, pallidum; orange, diencephalon; purple, midbrain; yellow, pons.

Figure 4.2 presents the heatmap obtained for the neurotransmitters acetylcholine, glutamate, norepinephrine, serotonin, dopamine and GABA. The concentrations of each metabolite per region are detailed in Tables S8-12. The brain regions were ordered using the distance from the bregma coordinates, starting with the positive distances on the left, to negative distances on the right. A distinct pattern was identified in the concentration of neurotransmitters across the rat brain. For example, regions within the brainstem have a low concentration of acetylcholine and glutamate, while a higher concentration of serotonin were measured in the raphe. Serotonin was more abundant in the substantia nigra (mean value 157.3 ± 77.6 ng/g wet brain tissue) compared to dopamine (mean value 145.2 ± 43.6 ng/g wet brain tissue). The serotonin/dopamine ratio had been documented and discussed before by Cragg, Hawkey, Greenfield [23] using fast-scan cyclic voltammetry with carbon-fibre microelectrodes. The substantia nigra receives serotonin innervations from the dorsal and medial raphe nuclei, providing input to dopaminergic dendrites. Interestingly, the frontal cortex has higher concentrations of acetylcholine and glutamate, while the olfactory bulb has a lower concentration in acetylcholine. The concentrations of dopamine and GABA are high across the midbrain which is consistent with the known distribution of dopaminergic neurons and GABAergic neuron projections within this area. Overall, the areas with the highest concentration of dopamine are the nucleus accumbens, caudate putamen and substantia nigra. The caudate putamen and substantia nigra are involved in the nigrostriatal pathway, which has a role in the regulation of movement where dopaminergic neurons are heavily involved. The nucleus accumbens, which is involved in the mesolimbic pathway, is another dopaminergic neuron projection dense region.

Comparison of brain regions along metabolic pathways

To demonstrate the applicability of the metabolic atlas in biochemical research, metabolite differences between selected brain regions were investigated along important metabolic pathways that are captured in the method. These brain regions are interlinked in their functionality, such as the regulation of movement (caudate putamen and substantia nigra) or are involved in similar health conditions, such as anxiety and post-traumatic stress disorder (amygdala, hypothalamus and infralimbic

cortex). The possibilities of utilising metabolic concentrations in biochemical interpretation are further expanded in the discussion.

Tyrosine metabolism

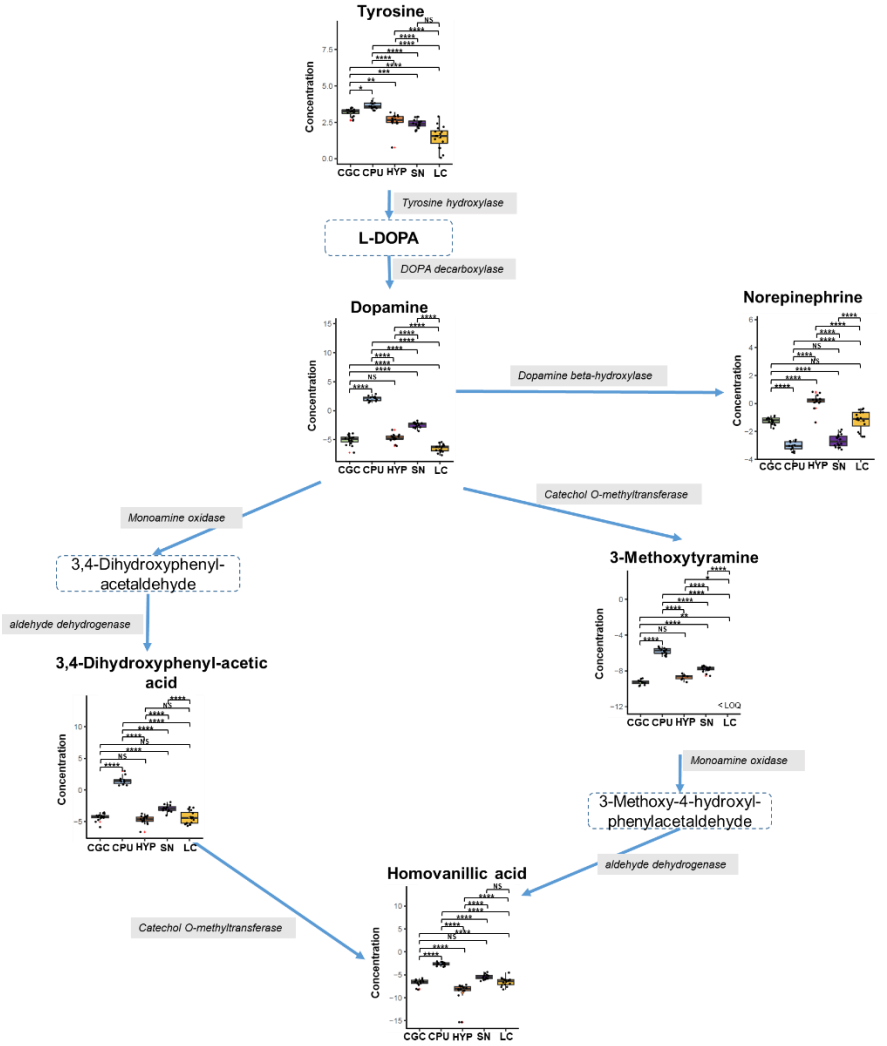

*Figure 4.3: Metabolite concentrations along the tyrosine pathway across five brain regions: cingulate cortex (CGC), caudate putamen (CPU), hypothalamus (HYP), substantia nigra (SN) and locus coeruleus (LC). Metabolite concentrations are expressed as log2 transformed values (ng/g wet brain tissue). The five brain regions were compared using one-way ANOVA followed by Tukey's HSD post-hoc test. Significance levels were ns = q > 0.05, * = q ≤ 0.05, ** = q ≤ 0.01, *** = q ≤ 0.001 and **** = q ≤ 0.0001.*

Seven metabolites in the tyrosine pathway were selected for this method, including the precursor tyrosine, its catecholamine neurotransmitter products, and a few of their degradation products as shown in Figure 4.3. Dramatic concentration differences were recorded for all metabolites between many of the selected brain regions. Tyrosine concentration was significantly different between most of the compared brain regions, decreasing from the caudate putamen through the hypothalamus, substantia nigra and, finally, the locus coeruleus. The concentration of dopamine was significantly higher in the caudate putamen and substantia nigra compared with the hypothalamus and locus coeruleus. The dopamine metabolites 3-MT, DOPAC and their metabolite HVA repeated the same pattern of differences between the brain regions. Moreover, the ratios describing the conversion into each product were reversed to the precursors in terms of relation between brain regions, apart from HVA/3MT which resembled the HVA. The above pattern recorded for 3-MT, DOPAC and HVA was the opposite to that of dopamine metabolites norepinephrine and epinephrine, showing higher metabolite levels in the hypothalamus and locus coeruleus, compared to the caudate putamen and substantia nigra. This suggests lower expression and activity of the enzyme dopamine β-hydroxylase, which metabolises dopamine to norepinephrine within the two regions. The turnover from dopamine to norepinephrine as depicted in a boxplot demonstrated not only a better within-region similarity, but also highlights the region with the highest turnover (LC).

Urea cycle and polyamine metabolism

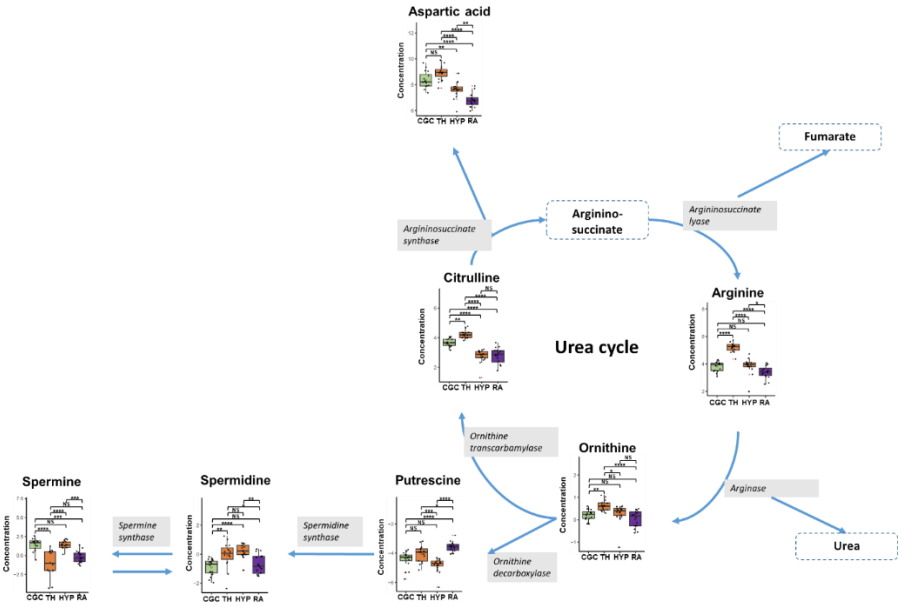

*Figure 4.4. Metabolite concentrations along the urea cycle and polyamine metabolism across four brain regions: (CGC), thalamus (TH), hypothalamus (HYP) and raphe (RA). Metabolite concentrations are expressed as log2 transformed values (ng/g wet brain tissue). The four brain regions were compared using one-way ANOVA followed by Tukey's HSD post-hoc test. Significance levels were ns = q > 0.05, * = q ≤ 0.05, ** = q ≤ 0.01, *** = q ≤ 0.001 and **** = q ≤ 0.0001.*

Figure 4.4 presents seven metabolite concentrations mapped along the urea cycle and polyamine pathway, across four brain regions spanning throughout the brain (prefrontal cortex, diencephalon and midbrain). A similar metabolic profile is observed across the four brain regions for the metabolites aspartic acid, arginine, citrulline and ornithine. However, there is a distinct change in metabolic ratios as ornithine exits the urea cycle to the polyamine metabolism. Here, we see the midbrain region raphe with a high concentration of putrescine. A rather striking observation is that the cingulate cortex showed a low concentration of spermidine but a high concentration of spermine. The opposite can be seen with the thalamus, which has a high concentration of spermidine but a relatively low concentration of

spermine. This difference can be explained by the reversible enzymatic conversion between spermine and spermidine.

Metabolic ratios

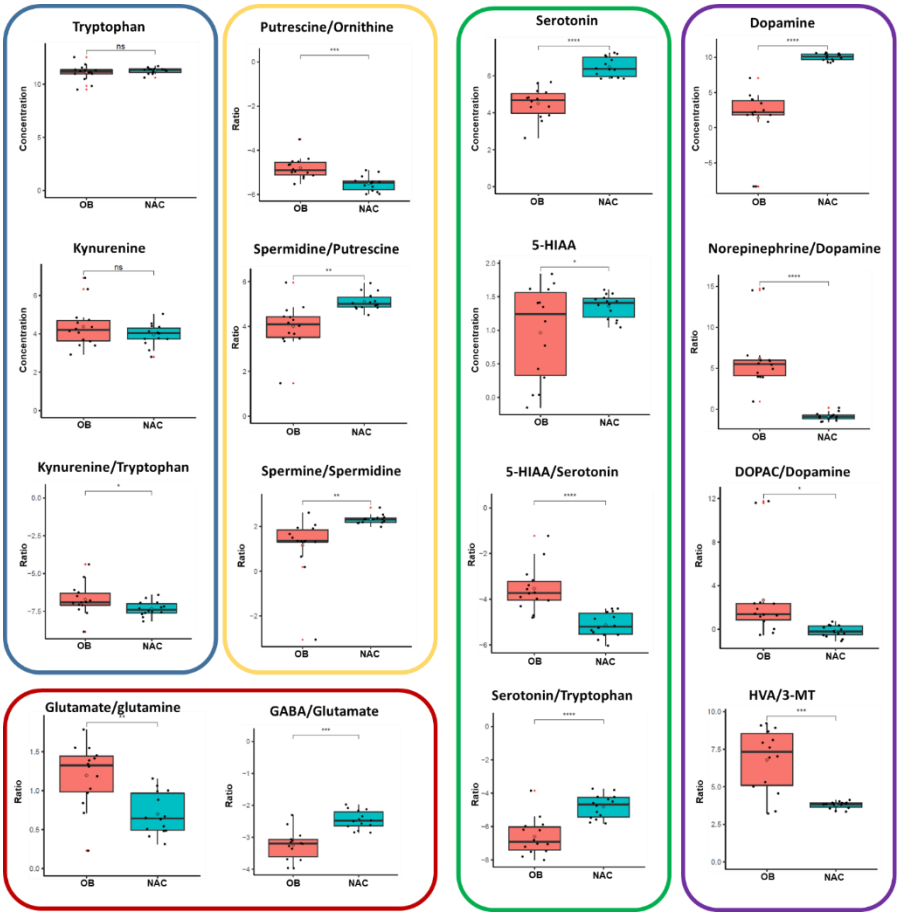

*Figure 4.5. Metabolic turnover ratios of metabolites captured in the olfactory bulb (OB) and nucleus accumbens (NAC). Metabolite concentrations are expressed as log2 transformed values (ng/g wet brain tissue). The data has been statistically compared using a paired t-test with Benjamini-Hochberg FDR correction. Significance levels were ns = q > 0.05, * = q ≤ 0.05, ** = q ≤ 0.01, *** = q ≤ 0.001 and **** = q ≤ 0.0001. The boxes indicate the metabolic pathways as follows: blue; tryptophan metabolism, yellow; polyamine metabolism, green; serotonin metabolism, purple; dopamine metabolism and red; GABA metabolism.*

An advantage of quantifying metabolites along the same pathway is the ability to estimate an enzymatic conversion between a precursor and a product even without

isotopically-labelled flux analysis. Of course, it should be taken into account that what might appear as conversion of a free amino acid into another might merely represent post-translational modification of an amino acid residue of a protein, followed by proteolysis. Therefore, we concentrated only on well-established direct conversions, such as the turnover of serotonin to 5HIAA, dopamine to norepinephrine and putrescine to spermidine. Based on the local expression of the converting enzymes, and the neuronal composition of different brain regions, we hypothesise that unique turnover ratios will be identified. These conversion rates must be calculated per animal and not from the mean of a group. Paired *t*-test with Benjamini-Hochberg FDR correction was calculated on the olfactory bulb and nucleus accumbens, as shown in Figure 4.5. Tryptophan and kynurenine are not significantly different, however when we evaluate the turnover ratio kynurenine/tryptophan, we see that there is a significant difference ($q = \leq 0.05$). This is a simple demonstration of how a ratio can portray significant differences that are not observed by the study of a single metabolite. Metabolic turnovers can also be used to reduce variation as seen with 5-HIAA in the olfactory bulb. When we look at the turnover ratio of 5-HIAA/serotonin, we have a reduced variation and greater significance ($q = \leq 0.0001$). The exit from the urea cycle to the polyamine pathway is shown with the ratio ornithine/putrescine, which is significantly greater in the olfactory bulb than in the nucleus accumbens ($q = \leq 0.001$). The polyamine turnover can then be explored using the ratios spermidine/putrescine and spermine/spermidine; both turnovers are lower in the olfactory bulb. Using the ratio GABA/glutamate, we can correlate this to the presence of glutamatergic or GABAergic neurons. We can also gather information regarding GABA synthesis by identifying the glutamate/glutamine ratio. Furthermore, this approach can be applied to the norepinephrine/dopamine ratio, which can be correlated to noradrenergic and dopaminergic neurons. The concentration of serotonin is lower in the nucleus accumbens compared to the olfactory bulb ($q = \leq 0.0001$). However, the turnover of serotonin to 5-HIAA by the enzyme monoamine oxidase is higher in the olfactory bulb ($q = \leq 0.0001$). In addition, this enzyme activity of monoamine oxidase can also be observed in the turnover of dopamine to DOPAC ($q = \leq 0.05$) and 3-MT to homovanillic acid ($q = \leq 0.001$).

Discussion

The presented study generated a quantitative neurochemical atlas of adult rat brain using an absolute quantitative methodology. Here, we objectively explore various brain regions ranging from the frontal cortex to the brainstem, of which each has specific roles, to allow exploration of regulatory functions and further associations with neurological diseases and psychiatric disorders.

As discussed earlier, the quantitation of neurochemicals is specifically challenging due to their broad range of physicochemical properties, chemical instability of neurotransmitters, and low concentrations requiring higher sensitivity. With the use of advanced techniques, as with the demonstrated pre-column derivatization followed by UHPLC-MS/MS analysis, it is possible to achieve accurate and reliable quantitation of the metabolic composition of each brain region. There were previous attempts to measure the healthy mammalian brain, although with limited metabolic coverage or brain regional coverage, and without addressing the stability issues of neurotransmitters. For example, Chen et al. (2016)[24] investigated the metabolic profile of the whole brains from six 4-week-old C56BL6 mice, which is of limited value for understanding the diversity and complexity across the brain. Nevertheless, these results can be somewhat compared to our metabolic atlas by using the mean values across brain regions. Using all of the comparable metabolites, we saw a similar order of magnitude concentrations are observed for amino acids, which are essential components in all cells (Asn 7429 ± 68 vs. 5718 ± 3120; Gln 165,427 ± 10647 vs. 217,651 ± 108,235; Tyr 3966 ± 278 vs. 5714 ± 2969, all in ng metabolite per g wet tissue), and dopamine (137.52 ± 12.42 vs. 214.62 ± 681.87 ng/g wet tissue). After taking the mean values of the metabolite concentrations as quantified from each of the 25 brain regions, our standard deviations were larger due to the changes in metabolite abundance across the brain as seen in Figure 4.1. Kaplan et al. (2013)[25] studied specific metabolites across the healthy rat brain, profiling on broader parts, such as the entire prefrontal cortex, without separating it into distinct anatomical regions as we report in the metabolic atlas. Therefore, only direct comparison of parent regions can be conducted and this yields dissimilar values, yet the metabolic abundance profile shows likeness in a few cases (for example, DOPAC is reported at 84.1 ng/g wet tissue at the prefrontal cortex, and mean of the regions in the atlas is 52.2 ng/g wet tissue). The comparison of literature values to the metabolic atlas

reference concentrations is challenging due to the factors listed above. In addition, it is clear that research of such a complex and diverse organ as the brain, requires that metabolites are quantified on a more localised and region-specific basis. Brain regions have their own distinct biological function, such as the cingulate cortex role in endocrine function, emotional learning and motivation [26], and the granular insular cortex role in visceral sensory function [27]. Moreover, different brain regions are associated with different diseases, such as the cingulate cortex association with schizophrenia and depression [28], and the infralimbic cortex association with anxiety and post-traumatic stress disorder [29].

The metabolic atlas provides distinct neurochemical profiles of brain regions, with some similarity between regions that share neighbouring anatomical location and neuronal pathways (for example, in regions of the cortex; agranular, dorsal and granular insular cortexes). It is clear that metabolic pathways, such as the tyrosine metabolism, urea cycle and polyamine metabolism, are differentially expressed. A clear evidence is the high concentrations of dopamine in brain regions that are known to have a high proportion of dopaminergic innervation. These regions include the caudate putamen and substantia nigra, which are part of the nigrostriatal pathway involved in the regulation of movement and associated with diseases such as Parkinson's [23,30,31]. The metabolic atlas can also provide biochemical insights via metabolic correlations that are associated with human health and disease. Two amino acids, β-alanine and arginine, positively correlate in most regions with neurotransmitters, GABA and choline, respectively. The relationship between β-alanine and GABA is well documented and has been shown in the cerebellum, specifically in Purkinje cells [32], and across the majority of the brain regions [20]. The metabolic atlas also showed that β-alanine correlated with dopamine in the nucleus accumbens, consistent with the report by Ericson et al (2010) [33]. A distinct dipeptide is carnosine, which measured high levels in the olfactory bulb, also aligns with Margolis et al (1974)[34] and Sharma et al (2015)[35] who reported that carnosine synthase I is expressed at a high level in the olfactory bulb. Interestingly, metabolic pathways such as the polyamine metabolism can also be used as biomarkers for brain trauma and stroke [36,37]. Although polyamine metabolism has a crucial role in cellular homeostasis and ROS scavenging, the full mechanism is still not totally understood [38].

The metabolic atlas can also be utilised to crudely outline the type of neurons that are present in the different regions of the brain, for example, the presence of acetylcholine and epinephrine prove the existence of cholinergic and adrenergic neurons. Furthermore, this can be correlated with genomics [39], transcriptomics [40] and proteomics [35] data that have been mapped in murine atlases. Various types of cells exist across brain regions, including glial cells and neurons. The presented metabolic atlas includes representative neurotransmitters that are produced or affected by the different neurons: acetylcholine (cholinergic neurons), dopamine (dopaminergic), norepinephrine (noradrenergic), GABA (GABAergic), glutamate (glutamatergic) and serotonin (serotonergic neurons). Brain regions and neuron cell types are associated with different CNS diseases and psychological conditions, including Alzheimer's disease, Attention Deficit Hyperactivity Disorder, addiction, depression, Huntington's disease and Parkinson's disease [41-44]. These illnesses can be related to specific regions and neuron cell types or distributed broadly across the brain. Therefore, the breadth of coverage of the metabolic atlas enables integration into systems biology-based models, such as genome-scale constraint-based models, to further understand the connectivity and function of the brain and, in turn, diseases [45,46].

Within the two pathways highlighted in our work, the tyrosine metabolism and urea cycle combined with polyamine metabolism demonstrate the ability to categorise regions based on presumed neuron abundance. For example, higher dopamine concentration in comparison to norepinephrine and epinephrine concentrations, suggests a region that is rich in dopaminergic neurons that express the enzyme tyrosine hydroxylase but lack the enzyme dopamine β-hydroxylase, which converts dopamine into norepinephrine [22]. However, adrenergic neurons contain both enzymes, producing dopamine as well as norepinephrine and epinephrine. There are higher levels of dopaminergic neurons and dopamine in the midbrain, controlling functionalities such as movement and emotional regulation (motivation, impulsiveness and pleasure). Lower concentration of dopamine were recorded in the hypothalamus (Fig 4.3), which governs hormonal regulation. In the regions of the Pons, such as locus coeruleus, we see a low concentration of dopamine and a high concentration of norepinephrine. This coincides with the locus coeruleus being one of the main point of origin for noradrenergic neurons [47]. Within the supporting information, we also see that regions mainly associated with emotional regulation,

such as the raphe, which is governed by serotonergic neurons, show the same low abundance of dopamine. [48]. Here, we also see the second highest concentration of serotonin across all brain regions after the substantia nigra (shown in Tables S8-12). The above examples demonstrate the application of neurotransmitter profiling to characterise the brain connectome. Similarly, mapping of metabolites along the urea cycle and polyamine metabolism can assist in understanding the biochemistry of the brain, as perturbations in these metabolites were associated with neurological disorders: stroke [36], Huntington's disease [49,50], and Alzheimer's disease [51].

Interestingly, by gauging the metabolic ratios between certain metabolites within this method, we can start to form correlations to pathway activation and enzyme function. Our findings show that a single metabolite does not always identify significant differences between regions in subtle pathways, like the tryptophan metabolism where the metabolite has more than one function; however, we can identify differences when we explore the metabolic ratio. The metabolic ratios can evaluate precursor metabolites involved in the synthesis of neurotransmitters such as GABA. GABA can be synthesised from two pathways, the polyamine degradation pathway [52,53] and the GABA shunt [54]. GABA is formed from both spermidine and putrescine via the enzymes diamine oxidase and polyamine oxidase, respectively, through the intermediate 4-aminobutyraldehyde [52]. At the same time, it is produced by glutamate via the enzyme glutamate decarboxylase [54]. This highlights the importance of understanding the urea cycle and polyamine metabolism when exploring the functions and presence of neurotransmitters. This is also seen with the formation of glutamate from glutamine or the TCA cycle. To expand understanding of the GABA shunt, the method by Willacey et al (2019)[55] can be used in the future as this quantitatively captures the TCA cycle. In the nucleus accumbens, we see a higher concentration of GABA and, in turn, we see a higher turnover of glutamate to GABA. Metabolic ratios can be predicted using metabolites that share the same enzyme as shown with the metabolites that share the enzyme monoamine oxidase.

The evaluation of neuronal health and communication can be accelerated by metabolic models that integrate omics data. Moreover, the study of the intracellular metabolic content and the extracellular environment would provide further information relating to the connectivity of brain regions. The metabolic atlas of the brain regions includes the concentrations of important metabolites, reflecting only

the intracellular metabolic content without distinguishing between synaptically transmitted neurotransmitters. A clear limitation of this approach is the absence of indication whether the presence of intracellular neurotransmitters correlates with extracellular synaptic release. Nevertheless, the high abundance of neurotransmitters in the brain regions suggests high likelihood that it is involved in neurotransmission. There are metabolomics approaches that can circumvent this issue of neurotransmission evaluation by measuring microdialysate [56,57] or CSF [58]. These approaches have their own limitations, in the form of low concentrations that requires high instrumental sensitivity, and the chemical instability of the targets under the analytical conditions with adequate derivatization of the vulnerable functional groups.

Quantitatively mapping the metabolic concentrations across the mammalian brain provides the scientific community with important reference data to support the interpretation of homeostasis and neuronal communication. Furthermore, the reference data can help in the identification of perturbations in the metabolic profile of murine models as a response to various CNS conditions. Of course, this needs to be further adapted and translated into human models, as the physiology differs. Analytically, the neurochemical reference values can assist in benchmarking method performance, and encouraging integration into genome-scale metabolic models. Utilising metabolomics in a quantitative fashion, which has been described as "the final piece in the omics puzzle", enables exploration of the brain architecture and function throughout these dynamic networks [4,8,59].

Materials and Methods

Chemicals

All chemicals were purchased from Sigma-Aldrich (St. Louis, USA) unless stated otherwise. Table S4 shows the ChEBI IDs of all targeted metabolites. The LC-MS grade ACN was sourced from Actu-all Chemicals (Oss, The Netherlands) and de-ionised water was produced using a Merck Milli-pore A10 purification system (Raleigh, USA).

Standard solutions

Stock solutions of 3-methoxytyramine, acetylcholine, aspartic acid, β-alanine, choline, dopamine, epinephrine, γ-aminobutyric acid, histamine, homoserine,

homovanillic acid, kynurenine, 3,4-dihydroxyphenylacetic acid, ornithine, putrescine, serotonin (5-HT), spermidine, spermine, tryptophan and tyrosine were prepared using 1 mg in 1 mL of de-ionised water, vortexed and stored at −80 °C. Similarly, stock solutions of 2 mg/mL were made for 5-HIAA, arginine, asparagine, ethanolamine, leucine and norepinephrine; 5 mg/mL for carnosine, citrulline, glutamic acid, isoleucine, methionine, phenylalanine, proline, serine, taurine and threonine; 10 mg/mL for alanine, cysteine, glutamine, glycine, histidine, lysine and valine.

Sample collection of rat brain regions

Male Wistar rats (Charles River Laboratories, Germany) were treated as approved under the ethical guidelines for the care and use of laboratory animals and were approved by the local animal care committee (Regierungspräsidium Karlsruhe, Germany). Sixteen male rats with initial weight of 300-350 g were given a 12-hour light/dark cycle (9:00 – 21:00) and *ad libitum* access to food and water. At the selected time points (17 and 19.5 weeks), the rats were euthanised, brains were quickly removed, snap-frozen in isopentane at −40 °C, and stored at −80 °C. Coronal brain sections (100 µm) of all brain matter were generated using a cryostat (Leica Biosystems CM3050S) and were immediately dissected using micropunch tools with different dimensions depending on the area of interest (0.75-1.25 mm diameter, Stoelting). Table 1 summarizes in detail, which micropunch was used for the respective brain regions as well as the means tissue weight of all micropunched regions. Bilateral samples were obtained under a magnifying lens using anatomical landmarks from Paxinos, Watson [60].

Brain region	Punch	Mean brain weight [mg]
OB - olfactorius bulbus	black	15.6
CgC - cingulate cortex	red	25.6
PrlC - prelimbic cortex	red	14.5
ILC - infralimbic cortex	red	11.7
GI - granular insular cortex	yellow/red	14.0

Brain region	Punch	Mean brain weight [mg]
DI - dorsal insular cortex	yellow/red	13.7
AI - agranular insular cortex	yellow/red	14.5
NAC - nucleus accumbens	red	19.9
CPU - caudate putamen	black	50.6
S - septum	yellow	13.7
BNST - bed nucleus of stria terminalis	red	9.7
GP - globus pallidus	red	13.9
HYP - hypothalamus	red	15.4
CMA - amygdala (central/medial)	red	11.4
BLA - amygdala (basal/lateral)	red	20.9
HB - habenula	yellow	11.7
HC - hippocampus	red/black	45.4
CA1 - field CA1 of hippocampus	red	15.6
Th - thalamus	red/black	30.0
STh - subthalamic nucleus	yellow	10.6
SN - substantia nigra	yellow	11.5
VTA - ventral tegmental area	yellow	7.3
RA - raphe	yellow	8.7
LC - locus coeruleus	yellow	9.3
PONS - pontine nuclei	red	9.1

Table 1: Detailed description of micropunches used for every region and the mean tissue weight.

Sample preparation of rat brain regions

Liquid-liquid extraction

The protocol for liquid-liquid extraction was based on the original Bligh & Dyer protocol [61,62]. Freeze-dried brain samples were kept at −80 ºC until sample preparation. The whole sample preparation was performed on ice. To each brain sample, 400 µL MeOH and 125 µL H_2O were added, together with the stable-isotope-labelled metabolites 2-aminobutyric acid-d_6, 3-(4-hydroxy-3-methoxy)-ethyl-d_4-amine, alanine-$^{13}C^{15}N$, arginine-$^{13}C^{15}N$, asparagine-$^{13}C^{15}N$, aspartic acid-$^{13}C^{15}N$, beta-Alanine-D_4, epinephrine-D_3, glutamic acid-$^{13}C^{15}N$, glutamine-$^{13}C^{15}N$, glycine-$^{13}C^{15}N$, histamine-D_4, isoleucine-$^{13}C^{15}N$, leucine-$^{13}C^{15}N$, lysine-$^{13}C^{15}N$, methionine-$^{13}C^{15}N$, ornithine-D_6, serine-$^{13}C^{15}N$, threonine-$^{13}C^{15}N$, tryptophan-$^{13}C^{15}N$, tyrosine-$^{13}C^{15}N$ and valine-$^{13}C^{15}N$ as internal standards. Samples were homogenised using a bullet blender at speed 9 for 3 min, with 0.5 mm stainless steel beads (Next Advance, USA). Following homogenization, samples were centrifuged for 5 min at 800 x g at 4 °C (Eppendorf 5415r centrifuge, country) and 450 µL of the homogenate was transferred into new tubes (1.5 mL). To these new tubes, 460 µL chloroform, 250 µL H_2O and 60 µL MeOH were added. The samples were vortexed for 30 s and left on ice for 10 min, followed by centrifugation for 10 min at 2,000 x g at 4 °C. The top aqueous layer (450 µL) was removed from the samples and transferred into new tubes (0.5 mL Eppendorf vials). Derivatization took place immediately after to reduce metabolite degradation.

Derivatization

The derivatization protocol was adapted from Wong et al (2012)[21]. Rat brain supernatant was transferred into a fresh vial (200 µL) and dried using a Labconco SpeedVac concentrator (MO, United States). The dried samples were reconstituted in 10 µL H_2O whilst maintained on ice. To start the derivatization reaction, 10 µL of 100 mM sodium carbonate (pH 9.4) was added, followed by 10 µL of 2% benzoyl chloride in ACN (v/v), and vortexed immediately for 10 seconds triggering the spontaneous S_n1 reaction at room temperature. The reaction was quenched by the addition of 20 µL H_2O with 1 % sulphuric acid after 5 minutes. To the quenched mixture, 50 µL H_2O was added to reduce the organic content. The samples were vortexed again and transferred to a glass injection prior to LC-MS analysis.

Liquid chromatography-tandem mass spectrometry (LC-MS/MS) Analysis

Analysis of the brain samples was conducted using an Agilent infinity Class II 1290 UHPLC system (Agilent Technologies, Germany) coupled to an SCIEX QTrap 6500 mass spectrometer (SCIEX, Massachusetts, USA). Five microliters of sample were injected on a T3 HSS C18 column (1.0 x 100 mm, 1.8 µm; Waters Technologies, UK) kept at 30 °C. The autosampler was maintained at 10 °C. Mobile phase A consisted of water containing 10 mM ammounium formate and 0.1% formic acid (v/v), and mobile phase B was 100 % ACN. The flow rate was 100 µL/min and the gradient profile was as follows: initial, 0% B; 0.01 min, 15% B; 0.5 min, 17% B; 14 min, 55% B; 14.5 min, 70% B; 18 min, 100% B; 20 min, 100% B and 22 min, 0% B. The mass spectrometer was operated in positive ionization mode at the following conditions: temperature 600 °C, curtain gas pressure 30.0 psi, collision gas set on medium, ionization voltage 5500 V, ion source gas 1 pressure 60.0 psi, and ion source gas 2 pressure 50.0 psi. Data was acquired using selected reaction monitoring (SRM), as detailed in Table S5. The samples were analysed against an eight-point calibration line with a two-fold dilution between each point. Five system suitability tests were injected before each batch and compared before the data analysis was continued. Nine quality control samples made of the pooled supernatant were injected per batch every 8-10 samples.

Statistical analysis

SCIEX MultiQuant was used for integration of the chromatographic peaks, confirmed by manual inspection. All concentrations were calculated across the calibration curves. The calibration line linear ranges are documented in Table S2. With the integrated data, statistical analysis was performed using R (http://cran.r-project.org/). The calculation of specific concentrations was calculated in R after assessing all analytical data for accuracy and linearity. Due to the large number of samples in this study (25 brain regions per 16 rats), they were analysed by LC-MS/MS in 10 continuous batches. To ensure data quality within and across batches, replicates of a pooled brain samples were measured in each batch for further quality analysis. In addition, each batch contained an independent metabolite calibration line to improve quantitation of the neurochemicals. Using an in-house quality control tool, we assessed the variation in metabolite area ratios between batches. Metabolites that fell below the lower limit of detection (LLOQ) were replaced with

values using minimum imputing during statistical analysis. The minimum imputing value was calculated using the method LLOQ/3. Sample outliers were not removed from the presented data to provide a realistic documentation of the biological and method variation. Before further analysis, samples were normalised to the corresponding brain sample wet weight. For each metabolite, a one-way ANOVA followed by Tukey's HSD post-hoc test was conducted to compare between the brain regions per animal. In addition, comparison of metabolite concentrations between brain regions were conducted using Student's *t*-test. False-discovery rate (FDR) correction using Benjamini–Hochberg. PCA was performed after $\log_2$ transformation and scaling.

Data quality assessment

The performance parameters were repeatability, linear range and linearity and are detailed in Table S2. Metabolites with a quality control sample interday repeatability relative standard deviation (RSD) of the area ratio below 20% were retained, except for epinephrine (RSD = 27.5 %) and homoserine (RSD = 23.7 %). We compared rats that were 17 weeks old (n = 6) and 19.5 weeks old (n = 10). A Student's *t*-test was conducted followed by correction for multiple comparisons (Benjamini-Hochberg FDR). We could therefore confirm that the neurochemical concentration is not significantly different between the two ages represented in our study (FDR $q > 0.05$). This was true for all regions except the hippocampus, the field CA1 of the hippocampus, dorsal insular cortex and thalamus (Table S3). The hippocampus regions both had 15 metabolites identified as significantly different (FDR $q < 0.05$) with the majority consisting of amino acids; the dorsal insular cortex had choline and citrulline identified as significant, and the thalamus had 5-HIAA identified as significant. Overall, the results show that we have established an accurate methodology that can be used to quantitatively map the adult rat brain as a model for mammalian brain. After the assessment, 43 neurochemicals were identified in a reliable quantifiable concentration (metabolite ChEBI identifiers shown in Table S4).

Acknowledgements

The author expresses thanks to Elisabeth Röbel, CIMH, for dissecting the brains and Nanda Koopman at Leiden University for assisting in the analysis of the brain samples. This project was supported by the SysMedPD and Sybil-AA projects, with

both receiving funding from the European Union's Horizon 2020 research and innovation programme under grant agreement no. 668738 and 668863, respectively.

References

1. Burte F, Houghton D, Lowes H, et al. metabolic profiling of Parkinson's disease and mild cognitive impairment. *Mov Disord.* 2017.
2. Havelund JF, Heegaard NHH, Faergeman NJK, Gramsbergen JB. Biomarker Research in Parkinson's Disease Using Metabolite Profiling. *Metabolites.* 2017;7(3).
3. Graham SF, Holscher C, Green BD. Metabolic signatures of human Alzheimer's disease (AD): 1 H NMR analysis of the polar metabolome of post-mortem brain tissue. *Metabolomics.* 2014;10(4):744-753.
4. Ivanisevic J, Epstein AA, Kurczy ME, et al. Brain region mapping using global metabolomics. *Chemistry & biology.* 2014;21(11):1575-1584.
5. Kanehisa M. Toward understanding the origin and evolution of cellular organisms. *Protein Sci.* 2019;28(11):1947-1951.
6. Romero P, Wagg J, Green ML, Kaiser D, Krummenacker M, Karp PD. Computational prediction of human metabolic pathways from the complete human genome. *Genome Biology.* 2004;6(1):R2.
7. Noronha A, Modamio J, Jarosz Y, et al. The Virtual Metabolic Human database: integrating human and gut microbiome metabolism with nutrition and disease. *Nucleic acids research.* 2018;47(D1):D614-D624.
8. Vasilopoulou CG, Margarity M, Klapa MI. Metabolomic analysis in brain research: opportunities and challenges. *Frontiers in Physiology.* 2016;7:183.
9. Dumas M-E, Davidovic L. Metabolic phenotyping and systems biology approaches to understanding neurological disorders. *F1000prime reports.* 2013;5.
10. Rae C. Metabolomics in neuroscience and disease. In: Future Medicine; 2014.
11. Gonzalez-Riano C, Garcia A, Barbas C. Metabolomics studies in brain tissue: A review. *Journal of Pharmaceutical and Biomedical Analysis.* 2016;130:141-168.
12. Wishart DS, Feunang YD, Marcu A, et al. HMDB 4.0: the human metabolome database for 2018. *Nucleic acids research.* 2018;46(D1):D608-d617.
13. Psychogios N, Hau DD, Peng J, et al. The Human Serum Metabolome. *PLoS One.* 2011;6(2):e16957.

14. Wu L, Niu Z, Hu X, et al. Regional cerebral metabolic levels and turnover in awake rats after acute or chronic spinal cord injury. *The FASEB Journal.* 2020;34(8):10547-10559.
15. Salek RM, Xia J, Innes A, et al. A metabolomic study of the CRND8 transgenic mouse model of Alzheimer's disease. *Neurochemistry international.* 2010;56(8):937-947.
16. Pinto MCX, de Paiva MJN, Oliveira-Lima OC, et al. Neurochemical study of amino acids in rodent brain structures using an improved gas chromatography–mass spectrometry method. *Journal of Chemical Neuroanatomy.* 2014;55:24-37.
17. Nicholson JK, Holmes E, Kinross JM, Darzi AW, Takats Z, Lindon JC. Metabolic phenotyping in clinical and surgical environments. *Nature.* 2012;491(7424):384-392.
18. Noga MJ, Dane A, Shi S, et al. Metabolomics of cerebrospinal fluid reveals changes in the central nervous system metabolism in a rat model of multiple sclerosis. *Metabolomics.* 2012;8(2):253-263.
19. Trushina E, Dutta T, Persson X-MT, Mielke MM, Petersen RC. Identification of altered metabolic pathways in plasma and CSF in mild cognitive impairment and Alzheimer's disease using metabolomics. *PLoS One.* 2013;8(5):e63644.
20. Choi WT, Tosun M, Jeong H-H, et al. Metabolomics of mammalian brain reveals regional differences. *BMC Systems Biology.* 2018;12(8):127.
21. Wong JM, Malec PA, Mabrouk OS, Ro J, Dus M, Kennedy RT. Benzoyl chloride derivatization with liquid chromatography-mass spectrometry for targeted metabolomics of neurochemicals in biological samples. *J Chromatogr A.* 2016;1446:78-90.
22. Meiser J, Weindl D, Hiller K. Complexity of dopamine metabolism. *Cell Communication and Signaling : CCS.* 2013;11:34-34.
23. Cragg S, Hawkey C, Greenfield S. Comparison of serotonin and dopamine release in substantia nigra and ventral tegmental area: region and species differences. *Journal of neurochemistry.* 1997;69(6):2378-2386.
24. Chen J, Hou W, Han B, et al. Target-based metabolomics for the quantitative measurement of 37 pathway metabolites in rat brain and serum using hydrophilic interaction ultra-high-performance liquid

chromatography-tandem mass spectrometry. *Anal Bioanal Chem.* 2016;408(10):2527-2542.

25. Kaplan KA, Chiu VM, Lukus PA, et al. Neuronal metabolomics by ion mobility mass spectrometry: cocaine effects on glucose and selected biogenic amine metabolites in the frontal cortex, striatum, and thalamus of the rat. *Anal Bioanal Chem.* 2013;405(6):1959-1968.
26. Devinsky O, Morrell MJ, Vogt BA. Contributions of anterior cingulate cortex to behaviour. *Brain.* 1995;118(1):279-306.
27. Cechetto DF, Saper CB. Evidence for a viscerotopic sensory representation in the cortex and thalamus in the rat. *Journal of Comparative Neurology.* 1987;262(1):27-45.
28. Cotter D, Mackay D, Landau S, Kerwin R, Everall I. Reduced glial cell density and neuronal size in the anterior cingulate cortex in major depressive disorder. *Archives of general psychiatry.* 2001;58(6):545-553.
29. Giustino TF, Maren S. The Role of the Medial Prefrontal Cortex in the Conditioning and Extinction of Fear. *Frontiers in Behavioral Neuroscience.* 2015;9(298).
30. Mhyre TR, Boyd JT, Hamill RW, Maguire-Zeiss KA. Parkinson's Disease. *Sub-cellular biochemistry.* 2012;65:389-455.
31. Biggio G, Casu M, Corda M, Di Bello C, Gessa G. Stimulation of dopamine synthesis in caudate nucleus by intrastriatal enkephalins and antagonism by naloxone. *Science.* 1978;200(4341):552-554.
32. Yeh H, Moises H, Waterhouse B, Woodward D. Modulatory interactions between norepinephrine and taurine, beta-alanine, gamma-aminobutyric acid and muscimol, applied iontophoretically to cerebellar Purkinje cells. *Neuropharmacology.* 1981;20(6):549-560.
33. Ericson M, Clarke RB, Chau P, Adermark L, Söderpalm B. β-alanine elevates dopamine levels in the rat nucleus accumbens: antagonism by strychnine. *Amino Acids.* 2010;38(4):1051-1055.
34. Margolis FL. Carnosine in the primary olfactory pathway. *Science.* 1974;184(4139):909-911.
35. Sharma K, Schmitt S, Bergner CG, et al. Cell type– and brain region–resolved mouse brain proteome. *Nature Neuroscience.* 2015;18(12):1819-1831.

36. Testai FD, Gorelick PB. Inherited metabolic disorders and stroke part 2: homocystinuria, organic acidurias, and urea cycle disorders. *Archives of neurology.* 2010;67(2):148-153.
37. Zahedi K, Huttinger F, Morrison R, Murray-Stewart T, Casero RA, Strauss KI. Polyamine catabolism is enhanced after traumatic brain injury. *Journal of neurotrauma.* 2010;27(3):515-525.
38. Ha HC, Sirisoma NS, Kuppusamy P, Zweier JL, Woster PM, Casero RA. The natural polyamine spermine functions directly as a free radical scavenger. *Proceedings of the National Academy of Sciences.* 1998;95(19):11140-11145.
39. Lein ES, Hawrylycz MJ, Ao N, et al. Genome-wide atlas of gene expression in the adult mouse brain. *Nature.* 2007;445(7124):168-176.
40. Ortiz C, Navarro JF, Jurek A, Märtin A, Lundeberg J, Meletis K. Molecular atlas of the adult mouse brain. *Science Advances.* 2020;6(26):eabb3446.
41. Reinikainen KJ, Paljärvi L, Huuskonen M, Soininen H, Laakso M, Riekkinen PJ. A post-mortem study of noradrenergic, serotonergic and GABAergic neurons in Alzheimer's disease. *Journal of the neurological sciences.* 1988;84(1):101-116.
42. Koob GF, Sanna PP, Bloom FE. Neuroscience of addiction. *Neuron.* 1998;21(3):467-476.
43. Kalivas PW. Neurocircuitry of addiction. *Neuropsychopharmacology: the fifth generation of progress.* 2002;95:1357-1366.
44. Godwin-Austen RB, Smith NJ. Comparison of the effects of bromocriptine and levodopa in Parkinson's disease. *J Neurol Neurosurg Psychiatry.* 1977;40(5):479-482.
45. Brunk E, Sahoo S, Zielinski DC, et al. Recon3D enables a three-dimensional view of gene variation in human metabolism. *Nature biotechnology.* 2018;36(3):272.
46. Thiele I, Swainston N, Fleming RM, et al. A community-driven global reconstruction of human metabolism. *Nature biotechnology.* 2013;31(5):419-425.
47. Sara SJ. The locus coeruleus and noradrenergic modulation of cognition. *Nature reviews neuroscience.* 2009;10(3):211-223.

48. Huang KW, Ochandarena NE, Philson AC, et al. Molecular and anatomical organization of the dorsal raphe nucleus. *Elife.* 2019;8:e46464.
49. Bichell TJV, Wegrzynowicz M, Tipps KG, et al. Reduced bioavailable manganese causes striatal urea cycle pathology in Huntington's disease mouse model. *Biochimica et Biophysica Acta (BBA)-Molecular Basis of Disease.* 2017;1863(6):1596-1604.
50. Chiang M-C, Chen H-M, Lee Y-H, et al. Dysregulation of C/EBPα by mutant Huntingtin causes the urea cycle deficiency in Huntington's disease. *Human molecular genetics.* 2007;16(5):483-498.
51. Hansmannel F, Sillaire A, Kamboh MI, et al. Is the urea cycle involved in Alzheimer's disease? *Journal of Alzheimer's Disease.* 2010;21(3):1013-1021.
52. Seiler N. CHAPTER 8 - POLYAMINE METABOLISM AND FUNCTION IN BRAIN. In: Osborne NN, ed. *Selected Topics from Neurochemistry.* Amsterdam: Pergamon; 1985:147-165.
53. Seiler N. Catabolism of polyamines. *Amino Acids.* 2004;26(3):217-233.
54. Yogeeswari P, Sriram D, Vaigundaragavendran J. The GABA shunt: an attractive and potential therapeutic target in the treatment of epileptic disorders. *Current drug metabolism.* 2005;6(2):127-139.
55. Willacey CCW, Naaktgeboren M, Lucumi Moreno E, et al. LC–MS/MS analysis of the central energy and carbon metabolites in biological samples following derivatization by dimethylaminophenacyl bromide. *Journal of Chromatography A.* 2019:460413.
56. Gottas A, Ripel A, Boix F, Vindenes V, Morland J, Oiestad EL. Determination of dopamine concentrations in brain extracellular fluid using microdialysis with short sampling intervals, analyzed by ultra high performance liquid chromatography tandem mass spectrometry. *J Pharmacol Toxicol Methods.* 2015;74:75-79.
57. Cannazza G, Carrozzo MM, Cazzato AS, et al. Simultaneous measurement of adenosine, dopamine, acetylcholine and 5-hydroxytryptamine in cerebral mice microdialysis samples by LC-ESI-MS/MS. *J Pharm Biomed Anal.* 2012;71:183-186.
58. Han X, Min M, Wang J, et al. Quantitative profiling of neurotransmitter abnormalities in brain, cerebrospinal fluid, and serum of experimental

diabetic encephalopathy male rat. *Journal of Neuroscience Research.* 2018;96(1):138-150.

59. Ivanisevic J, Siuzdak G. The role of metabolomics in brain metabolism research. *Journal of Neuroimmune Pharmacology.* 2015;10(3):391-395.
60. Paxinos G, Watson C. *The rat brain in stereotaxic coordinates: hard cover edition.* Elsevier; 2006.
61. Bligh EG, Dyer WJ. A rapid method of total lipid extraction and purification. *Canadian journal of biochemistry and physiology.* 1959;37(8):911-917.
62. Sündermann A, Eggers LF, Schwudke D. Liquid Extraction: Bligh and Dyer. In: Wenk MR, ed. *Encyclopedia of Lipidomics.* Dordrecht: Springer Netherlands; 2016:1-4.

Supplementary information

Table S1. The relative standard deviation of metabolites from the pooled brain samples for quality control.

Metabolite	QC_{RSD} (%)	Metabolite	QC_{RSD} (%)
3-Methoxytyramine	10.4	Homoserine	23.7
3,4-Dihydroxyphenylacetic acid	13.0	Homovanillic acid	13.0
5-Hydroxyindoleacetic acid	9.3	Hypotaurine	5.2
Acetylcholine	7.6	Isoleucine	2.3
Alanine	3.1	Kynurenine	10.3
Arginine	6.1	Leucine	2.1
Asparagine	5.9	Lysine	2.8
Aspartic acid	6.5	Methionine	2.0
β -Alanine	5.4	Norepinephrine	5.4
Carnosine	7.4	Ornithine	8.2
Choline	8.3	Phenylalanine	3.1
Citrulline	8.5	Proline	10.9
Cysteine	13.5	Putrescine	4.2
Dopamine	9.3	Serine	5.3
Epinephrine	27.5	Serotonin	17.2
Ethanolamine	12.5	Spermidine	9.1
Gamma-Aminobutyric acid	2.8	Spermine	10.3
Glutamic acid	5.1	Taurine	7.8
Glutamine	4.8	Threonine	5.4
Glutathione	8.4	Tryptophan	2.8
Glycine	5.4	Tyramine	25.9
Histamine	14.2	Tyrosine	1.8
Histidine	7.6	Valine	2.0

Table S2. Analytical results showing the linear equation, linear range and R^2 value of the metabolites.

Metabolites	Linear equation	Linear range (µM)	R^2
3-Methoxytyramine	y = −0.017 + 0.59 × X	0 - 9.82	0.997
3,4-Dihydroxyphenylacetic acid	y = −5e−04 + 0.059 × x	0 - 10.14	0.99
5-Hydroxyindoleacetic acid	y = 0.02 + 0.017 × X	0 - 210	0.993
Acetylcholine	y = 0.01 + 0.09 × x	0 - 11	0.992
Alanine	y = 0.0049 + 0.01 × x	0 - 1122	1
Arginine	y = 0.0089 + 0.018 × x	0 - 475	1
Asparagine	y = 0.0015 + 0.012 × x	0 - 151	0.999
Aspartic acid	y = 0.0073 + 0.016 × x	0 - 75	0.998
Beta-Alanine	y = 0.00007 + 0.01 × x	0 - 224	1
Carnosine	y = −0.022 + 0.017 × x	0 - 221	0.997
Choline	y = 0.0043 + 0.024 × x	0 - 8.7	0.995
Citrulline	y = 0.0071 + 0.0041 × x	0 - 713	0.998
Dopamine	y = 0.0012 + 0.069 × x	0 - 23.4	0.999
Epinephrine	y = -0.0019 + 0.029 × x	0 - 6.00	0.997
Ethanolamine	y = −2.1 + 1 × x	0 - 410	0.997
Gamma-Aminobutyric acid	y = 0.01 + 0.017 × x	0 - 48.5	0.998
Glutamic acid	y = 0.00082 + 0.019 × x	0 - 340	0.999
Glutamine	y = −0.064 + 0.026 × x	0 - 1370	1
Glycine	y = 0.017 + 0.011 × x	0 - 2663	1
Histamine	y = 0.011 + 0.028 × x	0 - 27.2	0.994
Histidine	y = −0.41 + 0.039 × x	0 - 955	0.995
Homoserine	y = 0.005 + 0.0075 × x	0 - 84.0	0.997
Homovanillic acid	y = 0.00019 + 0.11 × x	0 - 22.0	0.998
Hypotaurine	y = 0.001 + 0.009 × x	0 - 620	1
Isoleucine	y = 0.015 + 0.046 × x	0 - 190	0.999
Kynurenine	y = 0.002 + 0.38 × X	0 -48.0	0.997
Leucine	y = 0.0055 + 0.0095 × x	0 - 76.2	1
Lysine	y = 0.0037 + 0.0093 × x	0 - 548	0.999
Methionine	y = −0.0072 + 0.06 × x	0 - 168	1
Norepinephrine	y = −0.00057 + 0.029 × x	0 - 23.72	0.996
Ornithine	y = 0.037 + 0.053 × x	0 - 29.7	0.999
Phenylalanine	y = −0.0026 + 0.18 × x	0 - 303	0.999
Proline	y = 0.015 + 0.03 × x	0 - 217	1

Metabolites	Linear equation	Linear range (µM)	R^2
Putrescine	y = −0.0044 + 0.31 × x	0 - 12.4	1
Serine	y = 0.17 + 0.024 × x	0 - 475	0.999
Serotonin	y = 0.0097 + 0.18 × x	0 - 9.5	0.994
Spermidine	y = −0.42 + 0.99 × x	0 - 27.5	0.994
Spermine	y = −0.051 + 0.33 × x	0 - 9.88	0.969
Taurine	y = −0.012 + 0.0092 × x	0 - 1598	0.998
Threonine	y = 0.04 + 0.0053 × x	0 - 840	0.999
Tryptophan	y = −0.016 + 0.064 × x	0 - 490	1
Tyrosine	y = 0.011 + 0.16 × x	0 - 552	1
Valine	y = −0.012 + 0.032 × x	0 - 854	1

Table S3. FDR corrected student t-test values comparing the metabolite concentrations in the brain regions between 17 and 19.5 week old rats.

	Agranular insular cortex	Amygdala (basallateral)	Amygdala (centralmedial)	Bed nucleus of stria terminal	Field CA1 of hippocampus	Cingulate cortex	Caudate putamen	Dorsal insular cortex	Granular insular cortex	Globus pallidus	Habenula	Hippocampus	Hypothalamus	Infralimbic cortex	Locus coeruleus	Nucleus accumbens	Olfactory bulb	Pontine nuclei	Prelimbic cortex	Raphe	Septum	Substantia nigra	Subthalamic nucleus	Thalamus	Ventral tegmental area
3-Methoxytyramine	0.98	0.64	0.99	0.78	0.41	0.9	0.99	0.65	0.96	0.42	0.95	0.03	0.93	1	0.61	0.99	0.62	0.6	0.98	0.88	0.67	0.84	0.96	0.87	0.56
3,4-Dihydroxyphenylacetic acid	0.98	0.54	0.99	0.23	0.28	0.8	0.99	0.66	0.43	0.69	0.95	0.78	0.76	1	0.61	0.99	0.99	0.6	0.99	0.11	0.26	0.97	0.79	0.68	0.56
5-Hydroxyindoleactic acid	0.98	0.39	0.99	0.28	0.57	0.9	0.99	0.67	0.97	0.8	0.99	0.75	0.76	1	0.61	0.99	0.62	0.73	0.98	0.81	0.26	0.84	0.54	0.03	0.56
Acetylcholine	0.59	0.89	0.99	0.76	0.31	0.8	0.99	0.12	0.95	0.4	0.99	0.78	0.99	1	0.61	0.79	0.83	0.78	0.98	0.86	0.26	0.95	0.5	0.78	0.67
Alanine	0.98	0.49	0.99	0.37	0.06	0.95	0.99	0.12	0.22	0.47	0.95	0.19	0.66	1	0.61	0.79	0.53	0.79	0.98	0.55	0.28	0.84	0.5	0.49	0.56
Arginine	0.59	0.39	0.99	0.19	0.1	0.86	0.99	0.41	0.2	0.35	0.95	0.03	0.66	1	0.61	0.79	0.53	0.6	0.98	0.57	0.26	0.84	0.5	0.92	0.56
Asparagine	0.59	0.39	0.99	0.17	0.03	0.9	0.99	0.22	0.45	0.35	0.95	0.03	0.66	1	0.61	0.79	0.53	0.6	0.99	0.68	0.26	0.84	0.5	0.66	0.56
Aspartic.acid	0.59	0.79	0.99	0.19	0.25	0.95	0.99	0.4	0.43	0.35	0.95	0.03	0.76	1	0.61	0.79	0.53	0.6	0.99	0.58	0.26	0.84	0.5	0.56	0.56
.aminopropanoic.acid	0.98	0.45	0.99	0.17	0.02	0.95	0.99	0.18	0.45	0.81	0.95	0.05	0.76	1	0.61	0.99	0.57	0.6	0.98	0.75	0.28	0.84	0.5	0.53	0.56
Carnosine	0.98	0.41	0.99	0.25	0.03	0.86	0.99	0.12	0.96	0.35	0.95	0.11	0.76	1	0.61	0.82	0.99	0.6	0.98	0.56	0.26	0.84	0.5	0.58	0.56
Choline	0.98	0.89	0.99	0.64	0.93	0.95	0.99	0.02	0.16	0.6	0.95	0.16	0.66	1	0.61	0.79	0.54	0.79	0.98	0.55	0.29	0.99	0.5	0.72	0.56
Citrulline	0.59	0.39	0.99	0.37	0.15	0.91	0.99	0.05	0.39	0.35	0.95	0.07	0.76	1	0.61	0.79	0.53	0.6	0.98	0.55	0.26	0.84	0.64	0.9	0.62
Dopamine	0.65	0.65	0.99	0.88	0.27	0.8	0.99	0.4	0.97	0.35	0.99	0.97	0.99	1	0.61	0.99	0.9	0.91	0.98	0.84	0.26	0.97	0.5	0.55	0.56
Epinephrine	NA	0.96	0.99	0.88	0.67	NA	NA	0.5	NA	0.6	0.95	NA	0.76	1	0.61	0.79	0.87	0.67	0.98	0.55	0.33	0.84	0.56	0.48	0.56
Ethanolamine	0.59	0.78	0.99	0.17	0.03	0.95	0.99	0.38	0.2	0.35	0.95	0.07	0.66	1	0.61	0.79	0.53	0.6	0.99	0.55	0.26	0.95	0.5	0.67	0.56
Gamma.Aminobutyric.acid	0.98	0.79	0.99	0.25	0.11	0.86	0.99	0.19	0.2	0.75	0.95	0.15	0.77	1	0.61	0.79	0.99	0.79	0.98	0.55	0.26	0.95	0.5	0.67	0.56
Glutamic.acid	0.66	0.84	0.99	0.28	0.27	0.95	0.99	0.65	0.53	0.28	0.95	0.1	0.97	1	0.61	0.79	0.99	0.67	0.98	0.55	0.26	0.94	0.5	0.37	0.56
Glutamine	0.98	0.49	0.99	0.23	0.25	0.9	0.99	0.12	0.43	0.35	0.95	0.04	0.76	1	0.61	0.79	0.56	0.6	0.98	0.55	0.26	0.95	0.5	0.32	0.56
Glycine	0.98	0.54	0.99	0.23	0.03	0.95	0.99	0.16	0.16	0.35	0.95	0.04	0.72	1	0.61	0.79	0.53	0.6	0.98	0.57	0.26	0.84	0.5	0.71	0.56
Histamine	0.72	0.49	0.99	0.69	0.41	0.37	0.99	0.77	0.97	0.35	0.95	0.78	0.97	1	0.61	0.79	0.62	NA	0.99	0.55	0.26	0.97	0.5	0.38	0.56
Histidine	0.66	0.39	0.99	0.17	0.02	0.9	0.99	0.4	0.2	0.52	0.95	0.03	0.66	1	0.61	0.79	0.53	0.6	0.99	0.55	0.26	0.84	0.5	0.93	0.56
Homoserine	0.66	0.39	0.99	0.63	0.41	0.86	0.99	0.5	0.2	0.35	0.95	0.7	0.76	1	0.77	0.79	0.53	0.62	0.63	0.55	0.29	0.84	0.5	0.44	0.56
Homovanillic.acid	0.66	0.39	0.99	0.76	0.5	0.9	0.99	0.96	0.97	0.35	0.95	0.83	0.66	1	0.61	0.79	0.9	0.6	0.99	0.55	0.52	0.84	0.69	0.09	0.66
Hypotaurine	0.72	0.39	0.99	0.6	0.03	0.86	0.99	0.75	0.53	0.35	0.95	0.97	0.66	1	0.61	0.79	0.53	0.6	0.98	0.64	0.26	0.84	0.5	0.94	0.56
Isoleucine	0.98	0.39	0.99	0.25	0.05	0.9	0.99	0.18	0.2	0.75	0.95	0.04	0.66	1	0.61	0.79	0.53	0.6	0.99	0.55	0.36	0.95	0.56	0.68	0.57
Kynurenine	0.59	0.68	0.99	0.49	0.93	0.86	0.99	0.38	0.97	0.92	0.95	0.06	0.76	1	0.9	0.79	0.54	0.6	0.98	0.55	0.8	0.94	0.5	0.37	0.56
Leucine	0.98	0.54	0.99	0.25	0.06	0.9	0.99	0.12	0.2	0.81	0.95	0.06	0.66	1	0.61	0.79	0.53	0.6	0.98	0.55	0.29	0.99	0.55	0.8	0.56
Lysine	0.59	0.39	0.99	0.19	0.05	0.49	0.99	0.74	0.96	0.35	0.95	0.03	0.66	1	0.61	0.79	0.53	0.6	0.98	0.56	0.26	0.84	0.5	0.23	0.56
Methionine	0.59	0.39	0.99	0.17	0.03	0.86	0.99	0.5	0.43	0.6	0.95	0.03	0.66	1	0.61	0.82	0.53	0.6	0.98	0.55	0.26	0.84	0.5	0.89	0.56
N.Acetylputrescine	0.98	0.49	0.99	0.6	0.93	0.16	0.99	0.38	0.43	0.81	0.95	0.19	0.76	1	0.61	0.79	0.53	0.78	0.98	0.55	0.28	0.95	0.71	0.58	0.56
Norepinephrine	0.98	0.4	0.99	0.17	0.07	0.99	0.99	0.43	0.96	0.69	0.95	0.16	0.76	1	0.61	0.99	0.53	0.6	0.98	0.75	0.26	0.94	0.5	0.61	0.56
Ornithine	0.98	0.39	0.99	0.69	0.17	0.9	0.99	0.12	0.2	0.58	0.95	0.06	0.76	1	0.94	0.79	0.53	0.8	0.98	0.81	0.45	0.84	0.55	0.97	0.56
Phenylalanine	0.65	0.49	1	0.17	0.03	0.9	0.99	0.22	0.21	0.6	0.95	0.03	0.66	1	0.61	0.79	0.53	0.6	0.99	0.55	0.26	0.84	0.5	0.92	0.56
Proline	0.66	0.39	0.99	0.23	0.02	0.86	0.99	0.22	0.26	0.7	0.95	0.04	0.66	1	0.61	0.79	0.53	0.6	0.98	0.55	0.27	0.84	0.54	0.59	0.56
Putrescine	0.98	0.39	0.99	0.31	0.11	0.86	0.99	0.79	0.96	0.81	0.95	0.48	0.76	1	0.61	0.79	0.83	0.79	0.99	0.55	0.66	0.95	0.69	0.8	0.95
Serine	0.82	0.39	0.99	0.28	0.03	0.86	0.99	0.18	0.55	0.35	0.95	0.85	0.66	1	0.61	0.79	0.53	0.6	0.99	0.55	0.28	0.84	0.5	0.5	0.56
Serotonin	0.9	0.98	0.99	0.49	0.51	0.95	0.99	0.5	0.55	0.35	0.95	0.78	0.76	1	0.65	0.79	0.83	0.78	0.98	0.89	0.29	0.84	0.55	0.69	0.56
Spermidine	0.74	0.64	0.99	0.17	0.18	0.9	0.99	0.75	0.45	0.35	0.95	0.75	0.76	1	0.61	0.79	0.83	0.6	0.98	0.78	0.29	0.84	0.5	1	0.56
Spermine	0.98	0.96	0.99	0.19	0.17	0.9	0.99	0.75	0.43	0.55	0.95	0.21	0.66	1	0.61	0.99	0.83	0.6	0.99	0.55	0.29	0.84	0.5	0.71	0.56
Threonine	0.98	0.45	0.99	0.25	0.19	0.9	0.99	0.38	0.55	0.35	0.95	0.1	0.72	1	0.61	0.82	0.53	0.6	0.98	0.75	0.28	0.84	0.5	0.98	0.56
Tryptophan	0.59	0.39	0.99	0.17	0.03	0.86	0.99	0.43	0.38	0.45	0.95	0.03	0.66	1	0.61	0.99	0.53	0.6	0.98	0.27	0.26	0.84	0.5	0.69	0.57
Tyrosine	0.59	0.39	0.99	0.17	0.03	0.86	0.99	0.5	0.74	0.35	0.95	0.03	0.66	1	0.61	0.99	0.57	0.6	0.98	0.55	0.26	0.84	0.5	0.18	0.56
Valine	0.98	0.39	0.99	0.29	0.08	0.86	0.99	0.38	0.43	0.79	0.95	0.07	0.66	1	0.61	1	0.53	0.6	0.98	0.55	0.36	0.94	0.56	0.97	0.57

Table S4. ChEBI identifiers for metabolites used in this method, including the metabolite class and associated pathways.

Metabolite	ChEBI ID	Metabolite Class	Pathway
3-Methoxytyramine	1582	Dopamine metabolite	Tyrosine metabolism
3,4-Dihydroxyphenylacetic acid	41941	Dopamine metabolite	Tyrosine metabolism
5-Hydroxyindoleacetic acid	27823	Serotonin metabolite	Tryptophan metabolism
Acetylcholine	15355	Neurotransmitter	Cholinergic
Alanine	16977	Amino acid	
Arginine	29016	Amino acid	Urea cycle and polyamine metabolism
Asparagine	17196	Amino acid	
Aspartic acid	22660	Amino acid and neurotransmitter	
Beta-Alanine	16958	Amino acid and neurotransmitter	
Carnosine	15727	Antioxidant	
Choline	15354	Acetylcholine precusor	Cholinergic
Citrulline	18211	Biogenic amine	Urea cycle and polyamine metabolism
Cysteine	17561	Amino acid and neurotransmitter	
Dopamine	18243	Neurotransmitter	Tyrosine metabolism
Epinephrine	33568	Neurotransmitter	Tyrosine metabolism
Ethanolamine	16000	Biogenic amine	
Gamma-Aminobutyric acid	16865	Neurotransmitter	GABAergic
Glutamic acid	18237	Amino acid and neurotransmitter	
Glutamine	18050	Amino acid and neurotransmitter precusor	
Glycine	15428	Amino acid and neurotransmitter	
Histamine	18295	Neurotransmitter	
Histidine	15971	Amino acid and histamine precusor	
Homoserine	15699	Amino acid	
Homovanillic acid	545959	Dopamine metabolite	Tyrosine metabolism
Hypotaurine	16668	Antioxidant	
Isoleucine	24898	Amino acid	
Kynurenine	16946	Biogenic amine	Tryptophan metabolism
Leucine	25017	Amino acid	
Lysine	18019	Amino acid	
Methionine	16811	Amino acid	
Norepinephrine	18357	Neurotransmitter	Tyrosine metabolism
Ornithine	15729	Biogenic amine	Urea cycle and polyamine metabolism
Phenylalanine	28044	Amino acid	
Proline	26271	Amino acid	
Putrescine	17148	Polyamine	Urea cycle and polyamine metabolism
Serine	17822	Amino acid (D-isomer neurotransmitter)	
Serotonin	28790	Neurotransmitter	Tryptophan metabolism
Spermidine	16610	Polyamine	Urea cycle and polyamine metabolism
Spermine	15098	Polyamine	Urea cycle and polyamine metabolism
Taurine	15891	Neurotransmitter	
Threonine	16857	Amino acid	
Tryptophan	27897	Amino acid	Tryptophan metabolism
Tyrosine	18186	Amino acid	Tyrosine metabolism
Valine	16414	Amino acid	

Table S5. Analytical parameters showing the product and precursor ions, collision energy, retention time, declustering potential and entrance/exit voltage for the metabolites and internal standards.

Metabolites	Precusor ion (m/z)	Product ion (m/z)	Retention time (min)	Collision energy (eV)	Entrance potential	Exit potential	Declustering potential
2-Aminobutyric acid-D_6	214	105	5.05	20	10	6	30
3-(4-hydroxy-3-methoxy)-ethyl-D_4-amine	276	105	7.48	20	10	6	30
3,4-Dihydroxyphenylacetic acid	394	105	14.87	20	10	6	30
3-Methoxytyramine	376	105	15.33	20	10	6	30
5-Hydroxyindoleacetic acid	313	146	11.2	20	10	6	30
Acetylcholine	146	87	1.08	15	10	6	30
Alanine	194	105	4.07	20	10	6	21
Alanine-$^{13}C^{15}N$	198	105	4.07	20	10	6	21
Arginine	279	105	3.1	35	10	12	41
Arginine-$^{13}C^{15}N$	289	105	3.1	35	10	12	41
Asparagine	237	105	3.09	37	10	6	26
Asparagine-$^{13}C^{15}N$	243	105	3.09	37	10	6	26
Aspartic acid	238	105	3.37	10	10	6	30
Aspartic acid-$^{13}C^{15}N$	243	105	3.37	10	10	6	30
Beta-Alanine	194	105	3.9	20	10	6	30
Beta-Alanine-D_4	198	105	3.9	20	10	6	30
Carnosine	331	110	2.96	20	10	6	30
Choline	104	60	0.87	20	10	6	30
Citrulline	280	105	3.36	20	10	6	30
Dopamine	466	105	16.8	27	10	6	51
Epinephrine	496	105	16.15	27	10	6	56
Epinephrine-D_3	499	105	16.15	20	10	6	30
Ethanolamine	166	105	3.41	20	10	6	30

Metabolites	Precusor ion (m/z)	Product ion (m/z)	Retention time (min)	Collision energy (eV)	Entrance potential	Exit potential	Declustering potential
Gamma-Aminobutyric acid	208	105	4.32	10	10	6	30
Glutamic acid	252	105	3.64	20	10	6	26
Glutamic acid-$^{13}C^{15}N$	258	105	3.64	20	10	6	30
Glutamine	251	105	3.2	20	10	6	30
Glutamine-$^{13}C^{15}N$	260	105	3.2	20	10	6	30
Glycine	180	105	3.47	17	10	12	11
Glycine-$^{13}C^{15}N$	183	105	3.47	17	10	12	11
Histamine	216	105	3.14	20	10	6	30
Histamine-D_4	220	105	3.14	20	10	6	30
Histidine	260	105	2.86	31	10	6	30
Homoserine	224	105	3.33	20	10	6	30
Homovanillic acid	304	105	11.76	20	10	6	30
Hypotaurine	214	105	2.86	20	10	6	30
Isoleucine	236	105	7.99	25	10	14	16
Isoleucine-$^{13}C^{15}N$	243	105	7.99	25	10	14	16
Kynurenine	417	122	11.93	20	10	6	36
Leucine	236	105	8.34	25	10	14	16
Leucine-$^{13}C^{15}N$	243	105	8.34	25	10	14	16
Lysine	355	188	7.55	20	10	6	30
Lysine-$^{13}C^{15}N$	363	194	7.55	20	10	6	30
Methionine	254	105	6.35	15	10	6	30
Methionine-$^{13}C^{15}N$	260	105	6.35	15	10	6	30
Norepinephrine	482	105	15.7	27	10	6	56
Ornithine	341	174	6.93	15	10	6	30
Ornithine-D_6	347	180	6.93	15	10	6	30
Phenylalanine	270	120	8.51	10	10	6	30

Metabolites	Precusor ion (m/z)	Product ion (m/z)	Retention time (min)	Collision energy (eV)	Entrance potential	Exit potential	Declustering potential
Proline	220	105	4.72	20	10	6	30
Putrescine	297	105	8.03	30	10	6	30
Serine	210	105	3.17	20	10	6	30
Serine-$^{13}C^{15}N$	214	105	3.17	20	10	6	30
Serotonin	385	264	14.87	20	10	6	100
Spermidine	458	162	10.65	20	10	6	71
Spermine	619.6	497	12.41	25	10	18	31
Taurine	230	105	3.03	10	10	6	30
Threonine	224	105	3.6	10	10	6	36
Threonine-$^{13}C^{15}N$	229	105	3.6	10	10	6	36
Tryptophan	309	159	8.72	10	10	6	30
Tryptophan-$^{13}C^{15}N$	322	171	8.72	10	10	6	30
Tyrosine	390	105	12.89	30	10	6	51
Tyrosine-$^{13}C^{15}N$	400	105	12.89	30	10	6	51
Valine	222	105	6.33	30	10	6	30
Valine-$^{13}C^{15}N$	228	105	6.33	30	10	6	30

Table S6. Calculation table showing the difference tyrosine metabolism concentrations between the regions Cingulate cortex (CGC), caudate putamen (CPU), hypothalamus (HYP), substantia nigra (SN) and locus coeruleus (LC) with one-way ANOVA using the posthoc test of Tukey, and paired t-test with FDR adjustment with Benjamini-Hochberg.

Variable	Comparison	Tukey HSD	T-test	FDR adj.
Tyrosine	CPU-CGC	0.0383802	0.000012	2.82E-05
Tyrosine	HYP-CGC	0.0065248	0.003537	0.004879
Tyrosine	SN-CGC	0.0002474	1.78E-07	6.7E-07
Tyrosine	LC-CGC	0	7.97E-09	4.56E-08
Tyrosine	HYP-CPU	0.0000002	1.22E-06	3.63E-06
Tyrosine	SN-CPU	0	1.03E-08	5.58E-08
Tyrosine	LC-CPU	0	5.21E-10	5.08E-09
Tyrosine	SN-HYP	0.867557	0.257104	0.286335
Tyrosine	LC-HYP	0.0000001	0.000132	0.000244
Tyrosine	LC-SN	0.000006	6.03E-05	0.000121
Dopamine	CPU-CGC	0	4.47E-12	1.34E-10
Dopamine	HYP-CGC	0.5993419	0.382896	0.413759
Dopamine	SN-CGC	0	4.17E-07	1.38E-06
Dopamine	LC-CGC	0.0000002	0.000972	0.00148
Dopamine	HYP-CPU	0	6.15E-14	5.27E-12
Dopamine	SN-CPU	0	3.05E-12	1.09E-10
Dopamine	LC-CPU	0	4.9E-17	2.1E-14
Dopamine	SN-HYP	0	2.87E-07	1.02E-06
Dopamine	LC-HYP	0	1.04E-05	2.52E-05
Dopamine	LC-SN	0	1.66E-12	6.48E-11
Norepinephrine	CPU-CGC	0	1.52E-10	2.04E-09
Norepinephrine	HYP-CGC	0	1.05E-06	3.17E-06
Norepinephrine	SN-CGC	0	6.68E-09	3.98E-08
Norepinephrine	LC-CGC	0.9999564	0.624624	0.65357
Norepinephrine	HYP-CPU	0	1.56E-11	3.04E-10
Norepinephrine	SN-CPU	0.2308768	0.056935	0.067473
Norepinephrine	LC-CPU	0	1.46E-07	5.66E-07
Norepinephrine	SN-HYP	0	9.47E-10	7.39E-09
Norepinephrine	LC-HYP	0	0.0001	0.000192
Norepinephrine	LC-SN	0	1.72E-05	3.87E-05
DOPAC	CPU-CGC	0	4.04E-12	1.33E-10

Variable	Comparison	Tukey HSD	T-test	FDR adj.
DOPAC	HYP-CGC	0.4760077	0.07036	0.082023
DOPAC	SN-CGC	0.0000039	2.59E-05	5.63E-05
DOPAC	LC-CGC	0.9992935	0.934282	0.943076
DOPAC	HYP-CPU	0	1.09E-14	1.17E-12
DOPAC	SN-CPU	0	2.79E-11	4.99E-10
DOPAC	LC-CPU	0	7.3E-10	6.27E-09
DOPAC	SN-HYP	0	6.79E-06	1.69E-05
DOPAC	LC-HYP	0.6260875	0.215665	0.2422
DOPAC	LC-SN	0.0000015	0.00052	0.000829
3-MT	CPU-CGC	0	2.67E-08	1.23E-07
3-MT	HYP-CGC	0.8492226	0.444833	0.475893
3-MT	SN-CGC	0.0000192	4.57E-05	9.48E-05
3-MT	LC-CGC	0.0019659	0.001997	0.002894
3-MT	HYP-CPU	0	1.16E-07	4.73E-07
3-MT	SN-CPU	0.0001365	3.81E-09	2.59E-08
3-MT	LC-CPU	0	7.31E-09	4.24E-08
3-MT	SN-HYP	0.0000003	0.000121	0.000228
3-MT	LC-HYP	0.0401984	0.131591	0.150541
3-MT	LC-SN	0	2.28E-07	8.38E-07
HVA	CPU-CGC	0	7E-11	1.11E-09
HVA	HYP-CGC	0.0000619	0.006398	0.00855
HVA	SN-CGC	0.0811306	0.000408	0.000659
HVA	LC-CGC	0.9986749	0.70737	0.732807
HVA	HYP-CPU	0	1.04E-06	3.16E-06
HVA	SN-CPU	0.0000009	6.84E-10	5.98E-09
HVA	LC-CPU	0	2.16E-09	1.6E-08
HVA	SN-HYP	0	0.00022	0.000383
HVA	LC-HYP	0.0000214	0.003306	0.004592
HVA	LC-SN	0.1498828	0.000205	0.000359

Table S7. Calculation table showing the difference in the urea cycle metabolism concentrations between the regions cingulate cortex (CGC), thalamus (TH), hypothalamus (HYP) and raphe (RA) with one-way ANOVA using the posthoc test of Tukey, and paired t-test with FDR adjustment with Benjamini-Hochberg.

Variable	Comparison	Tukey HSD	Paired T-test	FDR adj.
Aspartic acid	HYP-CGC	0.004077	0.00582947	0.009115
Aspartic acid	TH-CGC	0.0653043	0.03385037	0.044787
Aspartic acid	RA-CGC	0	6.9645E-06	2.07E-05
Aspartic acid	TH-HYP	0.0000007	0.00016906	0.000363
Aspartic acid	RA-HYP	0.0015311	0.00079501	0.001497
Aspartic acid	RA-TH	0	8.2037E-09	7.06E-08
Arginine	HYP-CGC	0.9972692	0.96499371	0.972533
Arginine	TH-CGC	0	1.42E-07	6.78E-07
Arginine	RA-CGC	0.0606083	0.00420978	0.006831
Arginine	TH-HYP	0	9.917E-06	2.87E-05
Arginine	RA-HYP	0.0374952	0.06026586	0.077356
Arginine	RA-TH	0	8.819E-09	7.34E-08
Citrulline	HYP-CGC	0.0000002	2.6051E-05	6.65E-05
Citrulline	TH-CGC	0.0030859	6.7557E-06	2.03E-05
Citrulline	RA-CGC	0.0000003	1.286E-05	3.65E-05
Citrulline	TH-HYP	0	2.5047E-07	1.08E-06
Citrulline	RA-HYP	0.9968472	0.70833689	0.758195
Citrulline	RA-TH	0	2.6866E-09	2.89E-08
Ornithine	HYP-CGC	0.9118277	0.66940796	0.722624
Ornithine	TH-CGC	0.004658	5.5294E-05	0.00013
Ornithine	RA-CGC	0.4497391	0.14030167	0.173195
Ornithine	TH-HYP	0.0288558	0.03103136	0.041482
Ornithine	RA-HYP	0.14963	0.15637509	0.190306
Ornithine	RA-TH	0.0000345	0.00017963	0.00038
Putrescine	HYP-CGC	0.1429626	0.02577924	0.035191
Putrescine	TH-CGC	0.2026575	0.17064441	0.20573
Putrescine	RA-CGC	0.000061	0.00020668	0.00043
Putrescine	TH-HYP	0.0006571	0.00208103	0.003603
Putrescine	RA-HYP	0	2.6379E-06	8.51E-06
Putrescine	RA-TH	0.038648	0.00430864	0.006948
Spermidine	HYP-CGC	0.0000593	1.2728E-06	4.56E-06

Variable	Comparison	Tukey HSD	Paired T-test	FDR adj.
Spermidine	TH-CGC	0.00434	0.00366133	0.006038
Spermidine	RA-CGC	0.8038884	0.42072138	0.465863
Spermidine	TH-HYP	0.6212349	0.2898807	0.338413
Spermidine	RA-HYP	0.0012834	0.00176518	0.003119
Spermidine	RA-TH	0.0495354	0.01420687	0.020251
Spermine	HYP-CGC	0.999999	0.711175	0.758195
Spermine	TH-CGC	0.0000004	0.00052039	0.001009
Spermine	RA-CGC	0.0004895	0.00044222	0.000871
Spermine	TH-HYP	0.0000004	0.00019483	0.000409
Spermine	RA-HYP	0.0004671	4.9895E-05	0.00012
Spermine	RA-TH	0.1879476	0.13648489	0.169294

Figure S1. Principal component analysis (PCA) of the 25 brain regions.

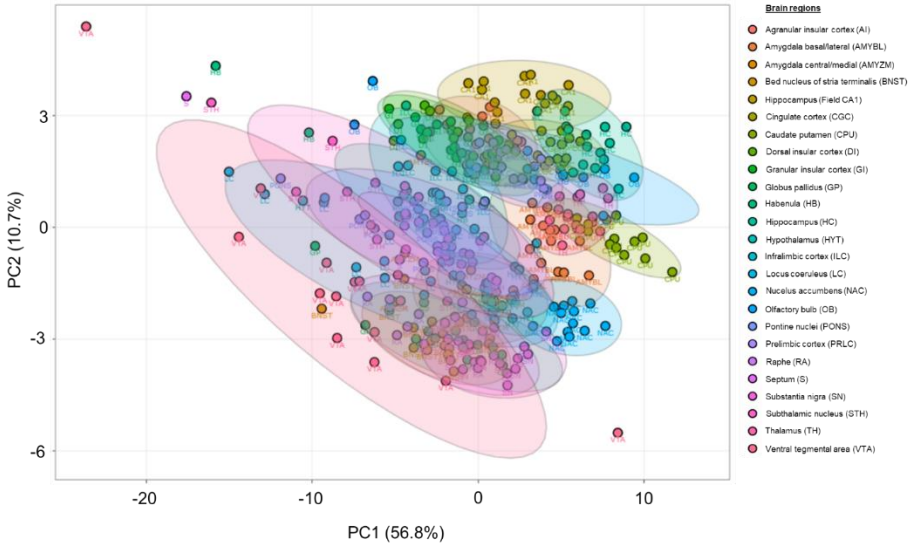

Figure S2. Neurochemical metabolome of healthy rodent brains (n = 16). The column represents each individual brain region and the row represents the metabolites quantified. The data has been clustered by brain region based on the metabolic profile similarity and the metabolites have been clustered based on their concentration similarity.

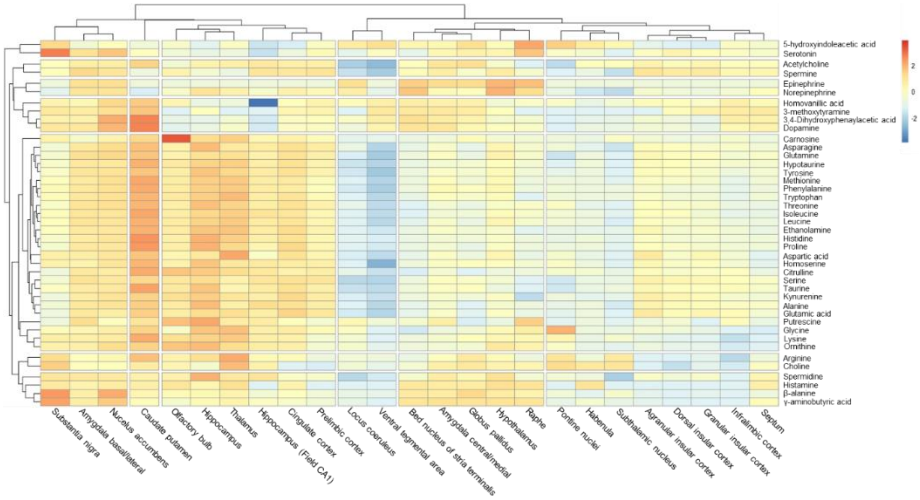

Table S8. Concentrations of metabolites from five brain regions: agranular insular cortex, amygdala (basal/lateral), amygdala (central/medial), bed nucleus of stria terminalis and field CA1 of hippocampus (ng/g wet tissue).

Metabolites	Agranular insular cortex	Amygdala (basal/lateral)	Amygdala (central/medial)	Bed nucleus of stria terminalis	Field CA1 of hippocampus
Acetylcholine	158.972 ± 24.9415	174.155 ± 39.054	185.96 ± 37.1674	135.215 ± 25.9035	183.979 ± 22.1108
Alanine	20420.7 ± 3000.06	27745.6 ± 5534.36	12358.5 ± 3026.47	8293.67 ± 1533.19	37355.7 ± 7680.86
Arginine	7912.27 ± 1965.3	13204.6 ± 3881.48	12753.8 ± 3601.68	9053.85 ± 2619.74	14307.8 ± 3212.39
Asparagine	5533.52 ± 1107.83	8400.29 ± 1974.44	4628.76 ± 1152.11	3359.36 ± 880.641	7788.9 ± 1882.06
Aspartic.acid	156605 ± 65421.6	165076 ± 43719.2	105205 ± 33867.7	67302.4 ± 19963.6	114678 ± 39944.2
Beta.Alanine	8.69351 ± 1.50709	23.9169 ± 5.77705	27.1273 ± 6.44169	28.1133 ± 9.93445	12.4067 ± 2.73043
Carnosine	885.961 ± 227.071	1045.15 ± 311.863	794.976 ± 161.697	636.325 ± 145.751	1589.97 ± 431.861
Choline	11719.6 ± 2473.44	17513.8 ± 4596.38	19086 ± 4513.93	16082.7 ± 4855.82	21496 ± 3550.78
Citrulline	9878.6 ± 2220.45	13390.7 ± 3931.37	7568.32 ± 2092.7	4476.52 ± 1087.49	13850.1 ± 2654.01
Dopamine	23.1735 ± 23.7747	164.397 ± 79.0223	190.337 ± 85.4983	216.385 ± 106.235	3.15742 ± 2.73132
Epinephrine	0.00034076 ± 0	0.982547 ± 1.08419	1.25766 ± 1.32894	2.64968 ± 2.2492	0.0531321 ± 0.186512
Ethanolamine	6257.54 ± 3168.77	10966 ± 4353.85	3608.02 ± 1282.28	1987.09 ± 664.009	10945.4 ± 5491.55
Gamma.Aminobutyric. acid	41746 ± 5418.05	77595.3 ± 16720.9	91444.4 ± 14538.5	84275.1 ± 17789.4	57793.2 ± 10301.5
Glutamic.acid	736144 ± 392360	727387 ± 191005	330401 ± 104720	202130 ± 57152.9	653966 ± 246743
Glutamine	230920 ± 38275.5	342059 ± 61039.7	188746 ± 40287.2	143678 ± 28532.6	254783 ± 54305.9
Glycine	21776.4 ± 4319.35	32165.5 ± 6902.9	18955.9 ± 3446.52	15036.5 ± 3576.7	34773.8 ± 8840.4
Histamine	1.21692 ± 4.86465	2.22502 ± 2.18496	7.53272 ± 5.47346	17.9942 ± 11.7084	1.86687 ± 7.46444
Histidine	5212.84 ± 1210.45	8547.77 ± 2416.86	4279.37 ± 924.335	3440.39 ± 744.522	7512.43 ± 2535.5
Homoserine	427.916 ± 72.2616	476.405 ± 134.768	350.479 ± 105.847	297.981 ± 103.374	453.063 ± 117.321
Homovanillic.acid	11.9776 ± 3.00515	15.0576 ± 6.38347	23.6929 ± 9.78977	35.5936 ± 19.8978	0.708928 ± 1.13577
Hypotaurine	3.15727 ± 0.864003	5.09547 ± 1.26089	2.13711 ± 0.585498	1.76199 ± 0.639967	3.78816 ± 1.32983
Isoleucine	1285.51 ± 207.054	1926.48 ± 450.082	1086.83 ± 279.511	823.099 ± 227.839	1846.84 ± 476.466
Kynurenine	15.321 ± 14.8495	14.0112 ± 5.18582	7.37899 ± 3.96571	4.15748 ± 1.99057	12.6655 ± 4.14046
Leucine	3652.08 ± 627.218	5607.22 ± 1207.15	3064.59 ± 679.56	2300.3 ± 597.798	4960.07 ± 1215.25
Lysine	9397.6 ± 2221	16010.7 ± 4576.26	11105.8 ± 2837.07	9157.32 ± 2803.19	14934.2 ± 3803.93
Methionine	2814.17 ± 617.602	4282.02 ± 1096.27	2757.01 ± 647.53	2093.83 ± 599.463	3832.48 ± 1106.7
Norepinephrine	206.77 ± 49.0701	493.129 ± 125.124	286.102 ± 66.389	875.249 ± 333.371	226.541 ± 73.7065
Ornithine	535.912 ± 222.989	784.573 ± 163.797	587.466 ± 234.835	494.206 ± 108.433	773.364 ± 146.277
Phenylalanine	3420.93 ± 714.569	5410.67 ± 1267.99	3697 ± 822.432	2777.68 ± 676.394	4984.75 ± 1315.41
Proline	4719.67 ± 981.488	9730.82 ± 2933.9	3354.54 ± 754.124	2498.81 ± 597.644	6355.83 ± 2527.52
Putrescine	19.1361 ± 7.89752	35.6063 ± 9.68012	27.5947 ± 8.14714	19.8089 ± 2.98606	31.1389 ± 10.4186

Serine	38670.5 ± 6291.33	54249.4 ± 11084.6	27767.1 ± 6489.08	18289.5 ± 3805.68	49072.9 ± 8563.71
Serotonin	38.2679 ± 24.9346	65.4906 ± 26.1903	40.4537 ± 16.8427	29.98 ± 20.9473	16.6772 ± 8.70513
Spermidine	450.204 ± 158.561	783.427 ± 314.482	660.419 ± 262.441	434.302 ± 193.06	851.082 ± 350.243
Spermine	3949.01 ± 1434.65	5033.21 ± 2438.55	2324.76 ± 1059.74	1252.03 ± 657.357	3325.73 ± 1331.4
Taurine	184744 ± 30803	254478 ± 64011.3	126910 ± 22588.4	87975.3 ± 19075.8	274284 ± 64513
Threonine	153861 ± 29368.8	231371 ± 49848.5	126249 ± 32667.4	95971.1 ± 21033.4	192283 ± 38836.6
Tryptophan	1515.45 ± 303.823	2344.07 ± 507.363	1543.86 ± 321.592	1170.63 ± 281.265	2118.63 ± 509.549
Tyrosine	5502.74 ± 1292.39	8277.86 ± 1888.76	4824.1 ± 1015.07	3689.18 ± 981.707	7358.29 ± 2027.42
Valine	2261.26 ± 397.93	3414.61 ± 807.676	1833.4 ± 471.546	1474.91 ± 357.103	3195.73 ± 796.129
3-Methoxytyramine	0.595814 ± 0.975758	2.83065 ± 0.834558	3.5757 ± 1.27649	3.99317 ± 0.865987	0.159074 ± 0.412127
3,4-Dihydroxyphenylacetic acid	35.8977 ± 21.1692	106.146 ± 52.7125	152.162 ± 58.0275	303.444 ± 112.566	7.16996 ± 3.58714
5-Hydroxyindoleacetic acid	1.85406 ± 0.421251	2.13679 ± 0.660286	3.0261 ± 0.595062	3.34928 ± 1.04111	1.2748 ± 0.1977

Table S9. Concentrations of metabolites from five brain regions: cingulate cortex, caudate putamen, dorsal insular cortex, granular insular cortex and globus pallidus (ng/g wet tissue).

Metabolites	Cingulate cortex	Caudate putamen	Dorsal insular cortex	Granular insular cortex	Globus pallidus
Acetylcholine	176.885 ± 34.2676	220.316 ± 38.8522	145.284 ± 37.7802	158.56 ± 28.4178	195.558 ± 50.0478
Alanine	31963.3 ± 5328.43	45741.6 ± 6919.51	17454.2 ± 3616.67	16642.5 ± 3769.31	7198.27 ± 2007.49
Arginine	12557.3 ± 2881.26	28727.4 ± 9177.13	6856.98 ± 1590.58	8028.89 ± 2132.5	18456.9 ± 8350.53
Asparagine	8976.77 ± 1152.61	11931.6 ± 2229.38	4972.42 ± 986.273	4542.75 ± 848.257	3140.12 ± 999.461
Aspartic.acid	242580 ± 121980	362283 ± 244582	111314 ± 46117.4	146252 ± 68956	85695.4 ± 37196.6
Beta.Alanine	16.5517 ± 2.01394	20.6594 ± 3.85917	8.08548 ± 1.80796	8.80726 ± 1.9214	38.5794 ± 11.6989
Carnosine	1857.78 ± 483.785	3561.17 ± 831.296	705.068 ± 135.926	730.884 ± 144.615	1267.5 ± 441.902
Choline	14205.4 ± 5407.54	35901.3 ± 33167.4	10264.2 ± 2579.23	11799.9 ± 3829.62	21887.7 ± 6311.49
Citrulline	11473.9 ± 2180.14	24606.9 ± 4650.7	8208.9 ± 1956.48	8826.9 ± 2219.82	4797.56 ± 1453.82
Dopamine	26.6111 ± 13.2396	3412.47 ± 1005.27	13.2417 ± 8.53102	8.17184 ± 5.16257	56.7327 ± 25.6333
Epinephrine	0.00034076 ± 0	0.00034076 ± 0	0.0349825 ± 0.138567	0.00034076 ± 0	1.25413 ± 1.07752
Ethanolamine	19710.7 ± 12927.7	40233.8 ± 27932.5	3673.43 ± 1618.68	4298.78 ± 2709.41	3017.49 ± 1391.75
Gamma.Aminobutyric.acid	54588.6 ± 8482.86	65634.3 ± 9007.05	37446.9 ± 6848.43	38884.5 ± 7335.29	92641 ± 24230.7
Glutamic.acid	1.15645e+06 ± 545507	1.17599e+06 ± 404705	447415 ± 109268	513937 ± 132330	190966 ± 96556.5
Glutamine	338799 ± 52711.3	451707 ± 93930.4	201162 ± 42228.5	190067 ± 32161.6	132075 ± 39174.6

Glycine	37058.5 ± 5700.22	52127.2 ± 11002	19521.4 ± 4012.77	17724 ± 4607.49	20421.2 ± 6463.02
Histamine	2.35283 ± 2.80255	2.81139 ± 0.980411	0.31583 ± 0.63934	0.310383 ± 0.794856	7.5352 ± 4.73455
Histidine	9963.9 ± 2310.46	23084.4 ± 4813.47	4506.48 ± 898.08	4301.96 ± 843.417	3649.81 ± 1271.82
Homoserine	454.695 ± 119.865	672.562 ± 174.082	344.634 ± 104.41	406.27 ± 81.5484	351.217 ± 156.268
Homovanillic.acid	9.82979 ± 3.79143	152.635 ± 39.3104	9.9473 ± 5.23554	6.83877 ± 3.23147	23.5218 ± 7.17038
Hypotaurine	5.48044 ± 1.26616	9.88593 ± 2.04759	2.60153 ± 0.666876	2.52763 ± 0.753303	1.91219 ± 0.675484
Isoleucine	1990.74 ± 344.357	3102.21 ± 568.966	1197.64 ± 313.193	1144.62 ± 325.459	990.836 ± 297.288
Kynurenine	23.87 ± 7.49545	25.3663 ± 9.29199	13.2583 ± 14.3705	10.5465 ± 6.12963	4.78938 ± 2.22949
Leucine	5628.27 ± 1076.45	8652.51 ± 1613.21	3158.88 ± 688.107	3120.35 ± 826.955	2674.87 ± 876.169
Lysine	14931.3 ± 3266.13	29567.5 ± 7676.46	8494.41 ± 2576.99	8279.85 ± 1941.02	13182.8 ± 4725.48
Methionine	4215.39 ± 902.402	7700.54 ± 1630.38	2442.53 ± 578.179	2496.47 ± 583.816	2644.49 ± 928.561
Norepinephrine	364.82 ± 59.6798	105.972 ± 23.0184	179.037 ± 48.7902	172.746 ± 37.139	263.374 ± 119.896
Ornithine	769.393 ± 130.63	1129.71 ± 230.296	513.932 ± 190.411	463.864 ± 127.389	499.881 ± 156.22
Phenylalanine	5085.28 ± 914.74	8516.99 ± 1678.68	2902.57 ± 615.635	2968.91 ± 710.085	3681.19 ± 1246.7
Proline	13589.1 ± 3635.66	28943.8 ± 5486.12	4008.8 ± 847.663	3737.96 ± 818.992	2581.04 ± 901.106
Putrescine	21.7945 ± 6.9398	31.9378 ± 7.61175	19.2621 ± 5.95057	15.5955 ± 4.46451	14.6196 ± 4.01968
Serine	53322.5 ± 8620.15	63921 ± 9616.6	33593.6 ± 6576.45	31969.7 ± 7382	23421.5 ± 7445.87
Serotonin	28.0253 ± 10.6664	34.3478 ± 7.99479	42.4078 ± 17.0353	36.9333 ± 11.5015	53.665 ± 27.2761
Spermidine	411.873 ± 147.486	627.91 ± 189.277	389.529 ± 142.548	441.358 ± 166.585	606.396 ± 350.322
Spermine	3064.93 ± 1440.93	577.772 ± 321.972	2821.81 ± 1154.71	2975.21 ± 1204.07	869.163 ± 490.549
Taurine	357446 ± 69998.6	879223 ± 166161	154259 ± 30812.6	142092 ± 24233.6	131377 ± 39774.3
Threonine	234543 ± 37766.3	340997 ± 56921.9	139802 ± 28815.6	133724 ± 30964.5	112650 ± 35887.5
Tryptophan	2380.93 ± 392.692	3775.72 ± 811.171	1325.92 ± 254.334	1358.2 ± 260.405	1532.75 ± 487.92
Tyrosine	8352.57 ± 1489.99	11941.8 ± 2612.9	4697.01 ± 1018.79	4610.54 ± 975.796	4552.55 ± 1419.19
Valine	3390.46 ± 506.811	4405.12 ± 716.511	2125.95 ± 587.514	1899.81 ± 543.598	1557.64 ± 393.828
3-Methoxytyramine	1.03721 ± 0.625142	15.4688 ± 3.70875	0.969123 ± 0.956178	1.24313 ± 0.970403	2.2528 ± 1.02326
3,4-Dihydroxyphenylacetic acid	44.6101 ± 14.1924	2584.21 ± 1447.61	20.8747 ± 7.77151	16.3223 ± 7.18972	95.7149 ± 35.999
5-Hydroxyindoleacetic acid	1.37456 ± 0.287738	2.01957 ± 0.48101	1.54948 ± 0.309255	1.50654 ± 0.280439	4.31572 ± 1.2141

Table S10. Concentrations of metabolites from five brain regions: habenula, hippocampus, hypothalamus, infralimbic cortex and locus coeruleus (ng/g wet tissue).

Metabolites	Habenula	Hippocampus	Hypothalamus	Infralimbic cortex	Locus coeruleus
Acetylcholine	138.168 ± 43.6301	165.02 ± 19.5724	124.348 ± 32.1786	131.279 ± 23.4067	76.8679 ± 34.4889
Alanine	9861.23 ± 3303.42	52040.5 ± 7740.68	12150.8 ± 2852.52	14341.1 ± 3074.6	7004.92 ± 3155.62
Arginine	9534.58 ± 2879.58	23889 ± 9208.28	13313.4 ± 4219.52	5315.42 ± 1131.98	10711.1 ± 5664.62
Asparagine	2872.13 ± 858.762	12577.7 ± 2458.18	5971.57 ± 1385.47	4610.16 ± 940.931	3085.58 ± 1297.01
Aspartic.acid	68398.6 ± 26941.6	197864 ± 76019.1	142104 ± 60497.4	88115.4 ± 25959.9	56901.5 ± 23118
Beta.Alanine	8.29832 ± 2.9573	21.4994 ± 3.37471	27.049 ± 6.90186	7.71419 ± 1.91731	10.0583 ± 4.09067
Carnosine	652.886 ± 198.304	3242.25 ± 708.84	901.386 ± 223.326	895.362 ± 211.056	568.995 ± 261.535
Choline	20588.8 ± 5609.09	23319.5 ± 21114.3	18593.6 ± 5101.23	11200.4 ± 2844.8	14378.6 ± 5234.86
Citrulline	7545.54 ± 3061.68	18059.4 ± 3371.51	6197.47 ± 1520.1	8894.43 ± 2256.46	9791.95 ± 15641.4
Dopamine	8.3133 ± 5.26903	11.0573 ± 11.0047	31.8595 ± 15.0168	66.4429 ± 54.6684	9.44439 ± 4.20101
Epinephrine	0.170341 ± 0.427837	0.00034076 ± 0	13.4651 ± 5.89928	0.286713 ± 0.789978	1.19952 ± 1.1403
Ethanolamine	1794.87 ± 704.67	24201.7 ± 10566	3519.15 ± 1380.41	2820.77 ± 1042.83	1281.98 ± 506.393
Gamma.Aminobutyric.acid	48111.1 ± 13335.7	66716.8 ± 8432.94	86435.7 ± 18729.2	40337.8 ± 8448.07	46304 ± 17958.8
Glutamic.acid	248042 ± 81758.8	913402 ± 219150	367987 ± 119743	449663 ± 139960	150508 ± 63147
Glutamine	136255 ± 42974.3	347705 ± 57770.3	240249 ± 61866.3	170557 ± 30971.1	100171 ± 38702.5
Glycine	18834.8 ± 5371.71	56089.1 ± 8057.97	28688.7 ± 7246.27	16321.9 ± 3877.35	27209.6 ± 11030.7
Histamine	31.9683 ± 31.3848	2.99243 ± 6.54254	49.7542 ± 19.7137	1.72495 ± 6.67775	0.165903 ± 0.482703
Histidine	3452.33 ± 955.246	17478.6 ± 4203.01	5234.3 ± 1333.36	3973.9 ± 814.586	3478.14 ± 3008.33
Homoserine	293.176 ± 106.317	675.657 ± 135.457	364.284 ± 95.8522	357.934 ± 102.212	278.106 ± 117.518
Homovanillic.acid	1.58565 ± 1.40712	1.88106 ± 1.39842	3.35833 ± 1.83234	25.2676 ± 9.34704	11.8782 ± 8.5344
Hypotaurine	2.10924 ± 1.14796	6.64859 ± 2.57326	2.87818 ± 0.834111	2.19391 ± 0.58954	1.6441 ± 1.75978
Isoleucine	973.13 ± 293.239	2445.6 ± 497.43	1415.99 ± 404.631	921.589 ± 239.288	940.536 ± 618.208
Kynurenine	3.77544 ± 2.5795	26.656 ± 13.8735	6.96688 ± 2.86564	7.00106 ± 2.68412	4.57299 ± 8.94593
Leucine	2581.96 ± 734.521	7312.12 ± 1380.91	4355.54 ± 1178.41	2569.87 ± 532.767	2374.01 ± 1275.1
Lysine	8745.92 ± 2804.35	23501.1 ± 6415.74	13573.9 ± 3968.45	6696.12 ± 1521.44	10181.5 ± 4238.08
Methionine	1890.51 ± 556.412	5895.08 ± 1447.09	3210.28 ± 931.119	1988.54 ± 444.251	1744.77 ± 885.39
Norepinephrine	103.54 ± 55.0668	566.341 ± 89.6003	999.84 ± 274.484	216.104 ± 51.1323	402.347 ± 168.232
Ornithine	461.006 ± 132.254	1141.85 ± 211.925	829.383 ± 178.856	441.306 ± 164.044	641.028 ± 472.706
Phenylalanine	2584.44 ± 737.314	7172.83 ± 1542.6	4249.39 ± 1215.51	2519.93 ± 481.125	2313.05 ± 1217.06
Proline	2635.07 ± 741.731	21375.3 ± 5036.44	4424.24 ± 1215.15	3291.85 ± 631.772	2129.14 ± 1192.86
Putrescine	19.7033 ± 7.63821	47.9962 ± 12.4828	16.3951 ± 4.22596	22.5052 ± 6.21627	26.3023 ± 11.6753
Serine	16937.4 ± 5651.8	53195.2 ± 18206.4	20693.6 ± 5828.76	28437.2 ± 6130.65	10340.4 ± 6168.73
Serotonin	33.3762 ± 21.9242	22.8848 ± 11.0523	46.0678 ± 25.7497	31.6357 ± 12.7856	41.7417 ± 39.7936

Spermidine	347.248 ± 160.279	1223.41 ± 325.251	893.652 ± 262.148	288.032 ± 114.994	216.448 ± 168.103
Spermine	675.306 ± 496.16	1103.67 ± 887.547	2864.24 ± 966.583	1943.31 ± 942.294	220.797 ± 183.648
Taurine	73285.3 ± 23928.4	567768 ± 113883	79730.1 ± 19118.2	146086 ± 28453.5	41047.1 ± 20256.7
Threonine	95874.2 ± 29435.3	308542 ± 53943.2	139969 ± 34226.8	115903 ± 23252.1	96878.6 ± 37932.1
Tryptophan	1148.85 ± 323.024	3249.14 ± 722.551	1755.03 ± 483.408	1142.61 ± 207.142	1071.82 ± 633.689
Tyrosine	3471.26 ± 1022.47	11146 ± 2308.85	5699 ± 1467.65	3975.1 ± 793.388	2887.27 ± 1498.56
Valine	1627.38 ± 503.157	4379.46 ± 661.883	2350.29 ± 612.083	1675.14 ± 429.542	1550.13 ± 861.186
3-Methoxytyramine	0.376592 ± 0.878296	0.516739 ± 0.411636	1.04471 ± 1.05857	1.82324 ± 1.57208	0.416013 ± 0.983928
3,4-Dihydroxyphenylacetic acid	15.0785 ± 6.45539	12.6215 ± 4.61137	34.4959 ± 13.2209	141.318 ± 114.406	51.2535 ± 37.9151
5-Hydroxyindoleacetic acid	3.63961 ± 1.13172	1.65129 ± 0.320298	2.91746 ± 0.907593	2.79776 ± 0.928344	3.77981 ± 1.52331

Table S11. Concentrations of metabolites from five brain regions: nucleus accumbens, olfactory bulb, pontine nuclei, prelimbic cortex and raphe (ng/g wet tissue).

Metabolites	Nucleus accumbens	Olfactory bulb	Pontine nuclei	Prelimbic cortex	Raphe
Acetylcholine	177.901 ± 38.4363	114.866 ± 33.275	88.4805 ± 27.41	173.629 ± 34.514	94.5811 ± 22.2539
Alanine	30622.9 ± 4853.34	26305.3 ± 11955.1	9020.19 ± 3447.32	24726.9 ± 4128.74	9117.19 ± 2247.88
Arginine	15653.4 ± 4481.52	17693.9 ± 9438.56	18867 ± 6296.07	9680.18 ± 2953.79	9628.19 ± 2934.15
Asparagine	9309.18 ± 1430.42	6685.86 ± 2837.42	3767.94 ± 1462.67	7623.51 ± 1217.04	4128.48 ± 1084.43
Aspartic.acid	197207 ± 62116.5	157733 ± 86537.9	95934.6 ± 36816.2	154405 ± 67457.4	78975.6 ± 31940.6
Beta.Alanine	63.7059 ± 11.4387	23.4305 ± 16.288	12.1537 ± 4.94786	11.6887 ± 1.80135	22.1656 ± 5.42069
Carnosine	1823.51 ± 330.184	31456.9 ± 34994.7	844.747 ± 325.997	1360.04 ± 256.101	822.183 ± 214.301
Choline	19272.3 ± 5167.82	20974.4 ± 7868.5	23828.7 ± 8682.65	12343.4 ± 3314.43	18952.6 ± 3337.13
Citrulline	12849.8 ± 2409.92	20322 ± 13201.4	8122.23 ± 3729.87	12022 ± 2271.01	6469.82 ± 2269.41
Dopamine	1085.77 ± 365.483	16.268 ± 34.3918	3.58438 ± 2.35233	32.1129 ± 25.6579	20.7751 ± 7.63125
Epinephrine	1.07023 ± 1.19154	0.32484 ± 1.02108	0.527166 ± 1.03566	0.000545216 ± 0.000791855	6.18125 ± 3.71557
Ethanolamine	12144.4 ± 5689.87	11490.7 ± 9701.95	2093.92 ± 796.816	8028.69 ± 4448.91	1764.76 ± 777.757
Gamma.Aminobutyric.acid	110943 ± 16336.1	57504.8 ± 25083.9	44691.8 ± 15833.9	50065.1 ± 8815.82	82140.8 ± 18093.8
Glutamic.acid	621347 ± 157150	552392 ± 247945	205776 ± 82744.7	730098 ± 205197	237309 ± 82670.2
Glutamine	372831 ± 51431.3	236507 ± 93195.3	95328.8 ± 28198.8	264763 ± 39769.9	164756 ± 45140.3
Glycine	35146.2 ± 6542.55	32443 ± 31899.2	64799.1 ± 23354.6	30047.3 ± 5871.53	36296.5 ± 9979.16
Histamine	5.80121 ± 2.69468	25.5235 ± 22.1847	24.1797 ± 0.000761343 ± 0	0.360308 ± 0.813683	15.9175
Histidine	9452.69 ± 2150.28	8869.12 ± 5357.03	3066.27 ± 1016.15	6491.57 ± 1350.95	3834.56 ± 991.668
Homoserine	489.315 ± 126.649	414.561 ± 122.392	398.272 ± 187.874	474.065 ± 141.103	360.217 ± 129.124
Homovanillic.acid	97.8893 ± 12.0437	19.1944 ± 13.3579	5.8841 ± 8.9546 ± 6.81338	18.3685 ± 3.80686	2.11213
Hypotaurine	5.09311 ± 1.11932	5.03698 ± 2.84029	1.36863 ± 0.515183	3.65632 ± 0.624271	2.0168 ± 0.677665
Isoleucine	1981.27 ± 492.631	2528.16 ± 2749.92	1085.43 ± 406.931	1583.9 ± 373.844	1104.41 ± 282.61
Kynurenine	16.3416 ± 6.37375	29.1928 ± 31.9169	2.46727 ± 5.1026 ± 3.98981	13.7396 ± 3.98437	2.2517
Leucine	5604.7 ± 1363.97	6857.12 ± 7071.86	3126.11 ± 2719.51 ± 885.8	4440.07 ± 1022.83	720.187
Lysine	16234.2 ± 3479.83	19241.1 ± 8299.96	15275.4 ± 7345.07	10882.4 ± 2097.39	13517.7 ± 4453.84
Methionine	4933.08 ± 1256.05	4897.32 ± 3925.76	2151.43 ± 848.416	3257.57 ± 690.664	2179.06 ± 635.242
Norepinephrine	584.528 ± 167.016	210.904 ± 76.3982	158.492 ± 62.8139	305.637 ± 48.4211	653.029 ± 182.841
Ornithine	1020.61 ± 219.81	1141.66 ± 428.869	617.457 ± 220.025	644.721 ± 296.96	691.672 ± 171.991
Phenylalanine	6083.03 ± 1284.09	6093.27 ± 5070.92	2766.18 ± 958.964	4132.51 ± 875.479	2741.37 ± 695.159

Proline	9782.41 ± 2568.14	11099.2 ± 8472.17	2522.08 ± 877.419	6815.52 ± 1494.58	2795.98 ± 723.041
Putrescine	22.7081 ± 4.4809	39.666 ± 10.9008	14.9952 ± 5.45182	21.6166 ± 6.54335	37.9712 ± 9.71125
Serine	44008.5 ± 7036.2	45363.1 ± 16938.1	11223.7 ± 3458.47	47151.2 ± 6757.2	12933.7 ± 2748.92
Serotonin	92.0468 ± 35.7517	25.9371 ± 13.0941	35.9664 ± 21.5807	37.8491 ± 12.3351	101.716 ± 64.708
Spermidine	807.423 ± 287.629	823.76 ± 675.48	403.971 ± 239.648	511.903 ± 198.303	493.291 ± 233.968
Spermine	4005.21 ± 1430.34	2078.06 ± 1631.89	340.641 ± 227.895	4667.23 ± 2009.88	1034.64 ± 619.939
Taurine	296200 ± 53220.6	284599 ± 136828	44648.4 ± 14484.5	227958 ± 36335	47910.5 ± 11950.5
Threonine	242927 ± 32228.5	192072 ± 81097.5	147749 ± 60371.1	194875 ± 39530.5	130205 ± 32486.1
Tryptophan	2557.7 ± 464.891	2474.95 ± 1288.68	1234.53 ± 401.369	1851.14 ± 339.05	1009.28 ± 255.505
Tyrosine	8413.53 ± 1493.66	7325.54 ± 3159.13	3318.82 ± 1296.67	6567 ± 1145.8	4036.74 ± 1028.79
Valine	3112.89 ± 570.189	3852.08 ± 3790.78	1806.05 ± 744.705	2739.9 ± 436	1962.56 ± 527.715
3-Methoxytyramine	7.12739 ± 1.62212	0.538299 ± 0.988628	0.172435 ± 0.46557	1.06161 ± 0.99864	1.18997 ± 1.77071
3,4-Dihydroxyphenylacetic acid	976.406 ± 270.726	25.4538 ± 32.9048	12.4972 ± 10.9419	60.2958 ± 27.7897	35.0891 ± 14.8275
5-Hydroxyindoleacetic acid	2.59312 ± 0.302986	2.16008 ± 0.935789	6.37339 ± 2.91409	2.49312 ± 0.556062	7.4911 ± 2.64128

Table S12. Concentrations of metabolites from five brain regions: septum, substantia nigra, subthalamic nucleus, thalamus and ventral tegmental area (ng/g wet tissue).

Metabolites	Septum	Substantia nigra	Subthalamic nucleus	Thalamus	Ventral tegmental area
Acetylcholine	135.554 ± 42.3912	141.364 ± 24.8703	147.818 ± 43.9152	173.287 ± 21.4608	87.7003 ± 94.8893
Alanine	12982.1 ± 3414.32	11216.5 ± 2175.87	6147.42 ± 2529.23	24493.6 ± 3423.05	5453.7 ± 5099.76
Arginine	8955.74 ± 3095.52	22585.8 ± 7192.26	17511.1 ± 7453.56	33030.1 ± 7671.21	10961.2 ± 8721.87
Asparagine	3768.94 ± 1120.7	4064.67 ± 776.878	2289.36 ± 916.053	7862.78 ± 898.556	2467.68 ± 2485.57
Aspartic.acid	64303.6 ± 27286.1	173167 ± 62940.6	67117.5 ± 36924.1	342326 ± 130637	57689.4 ± 48912.7
Beta.Alanine	11.2629 ± 3.35513	78.9253 ± 15.2423	13.8556 ± 6.93014	25.197 ± 7.89352	11.5286 ± 9.66957
Carnosine	662.783 ± 213.016	1806.23 ± 609.539	1150.36 ± 458.115	3676.51 ± 958.204	782.564 ± 753.096
Choline	15954.3 ± 4480.36	26730.9 ± 4838.69	21805.9 ± 8203.34	33531.4 ± 9603.52	16716 ± 20216.4
Citrulline	5770.69 ± 1642.02	6333.88 ± 1466.26	5743.94 ± 1994.69	16554.4 ± 3159.8	5046.36 ± 4650.74
Dopamine	77.1255 ± 35.6035	145.173 ± 43.5657	7.15894 ± 5.73189	22.2423 ± 13.7155	88.1404 ± 74.0207
Epinephrine	0.412285 ± 0.690775	0.403209 ± 0.764629	0.281557 ± 0.579828	0.436804 ± 0.665228	0.728507 ± 1.0525
Ethanolamine	2443.5 ± 1113.3	4634.79 ± 1884.06	2164.32 ± 1428.86	22680.5 ± 9248.76	1402.61 ± 1171.5
Gamma.Aminobutyric.acid	63074.4 ± 16469.4	134966 ± 20662.8	42328.5 ± 14926.8	74327.1 ± 9637.69	51478.4 ± 52295.4
Glutamic.acid	289570 ± 119812	297975 ± 107146	191460 ± 102379	954283 ± 284638	143840 ± 135923
Glutamine	170356 ± 50139	165700 ± 28467.8	108103 ± 44853.2	346080 ± 37137.8	87735.4 ± 82090.7
Glycine	14981.5 ± 4485.46	29182.5 ± 6364.23	18785.9 ± 6774.96	59092.2 ± 6508.26	19185.5 ± 16486.5
Histamine	3.62362 ± 4.05061	9.3332 ± 6.24084	3.78297 ± 6.11408	50.4631 ± 25.7226	10.05 ± 31.4831
Histidine	3650.09 ± 1006.2	4884.31 ± 1139.92	2900.89 ± 1014.16	12861.5 ± 2567.07	2960.27 ± 2513.82
Homoserine	310.669 ± 128.546	462.035 ± 128.848	283.443 ± 164.266	509.911 ± 50.1137	244.941 ± 207.314
Homovanillic.acid	14.0249 ± 6.49057	22.0263 ± 8.61756	4.33919 ± 3.44579	2.37363 ± 1.24548	34.0534 ± 28.8892
Hypotaurine	2.00881 ± 0.56206	2.35249 ± 0.620103	1.23895 ± 0.615422	7.18556 ± 1.51779	1.02985 ± 1.65152
Isoleucine	914.11 ± 254.46	1396.1 ± 322.424	808.772 ± 328.185	2591.02 ± 423.957	758.278 ± 728.869
Kynurenine	5.17378 ± 1.85068	15.4285 ± 41.1177	3.46619 ± 2.21863	15.0323 ± 7.25279	11.6354 ± 37.4386
Leucine	2501.34 ± 702.445	3689.04 ± 740.998	1937.21 ± 762.465	7361.63 ± 1343.01	1898.58 ± 1747.54

	7407.73 ±	18291.7 ±	11803.4 ±	25517.7 ±	8727.84 ±
Lysine	2234.78	4983.93	5161.64	5067.27	7420.91
		2889.94 ±	1696.12 ±	5907.28 ±	1490.79 ±
Methionine	2248 ± 673.652	749.116	801.627	1133.28	1448.39
	263.298 ±	139.279 ±	86.5197 ±	367.937 ±	190.817 ±
Norepinephrine	86.4125	44.258	47.7059	74.4545	195.356
	419.498 ±	744.614 ±	489.863 ±	1033.77 ±	532.557 ±
Ornithine	114.621	137.952	169.532	177.618	462.125
	2754.72 ±	4086.75 ±	2414.73 ±	7463.5 ±	1995.05 ±
Phenylalanine	830.157	938.891	1020.69	1280.36	1938.86
	2859.86 ±	3632.8 ±	1956.51 ±	13831.5 ±	1904.91 ±
Proline	824.756	862.246	828.304	3273.01	1848.16
	17.7438 ±	17.8071 ±	18.0273 ±	28.1669 ±	
Putrescine	5.64527	4.77939	10.107	10.7512	21.515 ± 11.8501
	24382.3 ±	21320.4 ±	16763.7 ±	38174.2 ±	9671.41 ±
Serine	7063.17	4478.35	5500.11	5858.35	8264.49
	29.2718 ±	157.249 ±	18.4931 ±	30.0821 ±	55.1209 ±
Serotonin	12.0165	77.5567	9.82114	16.9682	72.5741
	502.115 ±	776.144 ±	353.284 ±	810.628 ±	263.499 ±
Spermidine	235.007	296.104	437.31	419.101	157.306
	1654.02 ±	1112.98 ±	207.207 ±	875.303 ±	168.232 ±
Spermine	845.076	425.408	172.76	732.434	218.189
	114930 ±	137431 ±	80749.4 ±	215039 ±	43003.2 ±
Taurine	33681.4	27511.7	29851.1	46450.4	42608.9
	109252 ±	139060 ±	91888.6 ±	271433 ±	90372.6 ±
Threonine	32490.4	30663.2	32024.8	29823.2	92506.9
	1251.22 ±	1756.16 ±	1155.51 ±	3502.49 ±	
Tryptophan	383.286	382.713	471.815	469.987	916.966 ± 803.25
	3898.35 ±	4942.7 ±	2895.25 ±	9704.05 ±	
Tyrosine	1163.78	1040.97	1148.24	1238.91	2384.49 ± 2348
	1599.33 ±	2084.91 ±	1208.35 ±	3439.46 ±	1265.33 ±
Valine	434.511	441.15	405.322	385.001	1127.31
	2.90899 ±	3.77405 ±	0.515119 ±	0.535187 ±	4.01339 ±
3-Methoxytyramine	0.752505	0.740801	0.995858	0.542754	4.50581
3,4-Dihydroxyphenylacetic acid	102.334 ± 35.5321	117.232 ± 43.2602	15.8703 ± 8.03395	30.1396 ± 8.70261	173.8 ± 156.472
5-Hydroxyindoleacetic acid	2.14027 ± 0.555773	4.77231 ± 0.705951	2.96337 ± 0.870568	2.55508 ± 0.383124	5.45705 ± 4.59809